The effective nucleon axial mass approach and quasielastic neutrino event rates in NOνA and Super-Kamiokande

K. Kuzmin[ab], V. Naumov[a], O. Petrova[a], I. Shandrov[a], A. Sheshukov[a]

[a] Joint Institute for Nuclear Research,
[b] Institute for Theoretical and Experimental Physics

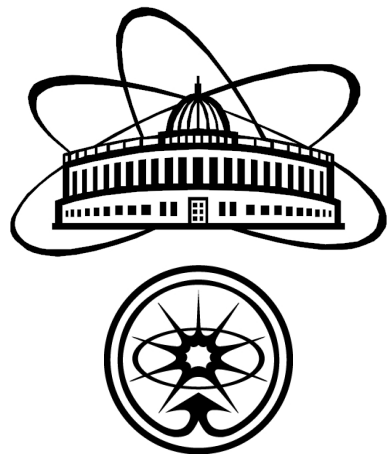

Outline

- The nucleon axial mass:
  - the problem
  - the solution concept: effective axial mass
- QES event rate calculation examples:
  - the Near Detector of NOνA
  - Super-Kamiokande
- Conclusions

QES of neutrino on the nucleon

QES section:

$$\boxed{d\sigma = \frac{G_F^2 M}{16\pi^2 (kp)} \left(1 + \frac{Q^2}{M_W^2}\right)^{-2} L^{\alpha\beta} W_{\alpha\beta} \frac{d^3\vec{k}'}{2k_0'}.}$$

Lepton tensor:

$$L^{\alpha\beta}(k,k') = \begin{cases} j^{\alpha}(k,k') j^{*\beta}(k,k') & \text{for } \nu; \\ \bar{j}^{\alpha}(k,k') \bar{j}^{*\beta}(k,k') & \text{for } \bar{\nu}. \end{cases}$$

Weak lepton currents:

$$j^{\alpha}(k,k') = \bar{u}(k')\gamma^{\alpha}\frac{1-\gamma_5}{2}u(k), \qquad \bar{j}^{\alpha}(k,k') = \bar{v}(k)\gamma^{\alpha}\frac{1-\gamma_5}{2}v(k').$$

Hadron tensor:

$$W_{\alpha\beta}(p,q) = \frac{1}{4}\int J_{\alpha}(p,p') J^{*}_{\beta}(p,p') \delta^4(k'+p'-k-p)\frac{d^3\vec{p}'}{2p_0'}.$$

Weak form factors of the nucleon

Weak hadron current is given by

$$J_\alpha(p,p') = V_{ud}^{\mathrm{CKM}} \bar{u}_p(p') \Gamma_\alpha(p,q) u_n(p).$$

Basis expansion of $\Gamma_\alpha(p,q)$ comes to

$$\Gamma_\alpha(p,q) = \gamma_\alpha F_V + i\sigma_{\alpha\beta}\frac{q^\beta}{2M} F_M + \frac{q_\alpha}{M} F_S + \\ + \left(\gamma_\alpha F_A + \frac{p_\alpha + p'_\alpha}{M} F_T + \frac{q_\alpha}{M} F_P\right)\gamma_5.$$

Standard dipole parametrization of the axial form factor is

$$F_A(Q^2) = g_A \left(1 + \frac{Q^2}{{M_A}^2}\right)^{-2}, \qquad g_A = -1.2695.$$

PCAC gives the formula for pseudoscalar form factor:

$$F_P(Q^2) = \frac{2M^2}{m_\pi^2 + Q^2} F_A(Q^2).$$

World survey of M_A

The current best-fit value (with 1σ and 2σ st. deviations) derived on hydrogen, deyterium and high-energy data[1]:

$$\boxed{M_A = 1.012 \pm 0.031 \left(^{+0.061}_{-0.06}\right) \text{GeV}.}$$

Experimental results:

NOMAD (with stat. and syst. errors)[2]: $M_A = 1.05 \pm 0.02 \pm 0.06$ GeV.

K2K[3]: $M_A = 1.2 \pm 0.12$ GeV.

MiniBooNE[4]: $M_A = 1.35 \pm 0.17$ GeV.

T2K shape-fit[5]: $M_A = 1.38 \left(^{+0.39}_{-0.27}\right)$ GeV.

[1] Kuzmin, Lyubushkin & Naumov, 2008; Kuzmin & Naumov, in preparation.
[2] Lyubushkin (NOMAD Collaboration), 2009.
[3] Gran (The K2K Collaboration), 2006.
[4] Aguilar-Arevalo *et al.* (The MiniBooNE Collaboration), 2010.
[5] Hadley (The T2K Collaboration), 2013.

MiniBooNE

The flux-weighted double differential cross sections for the $\nu_\mu n \to \mu^- p$ reaction.

The MiniBooNE result[1]: $M_A = 1.35 \pm 0.17\,\text{GeV}$.

The gray bands are calculated by using the nuclear model of Martini *et al.*[2].

Does the RFG model[3] work at low energies?

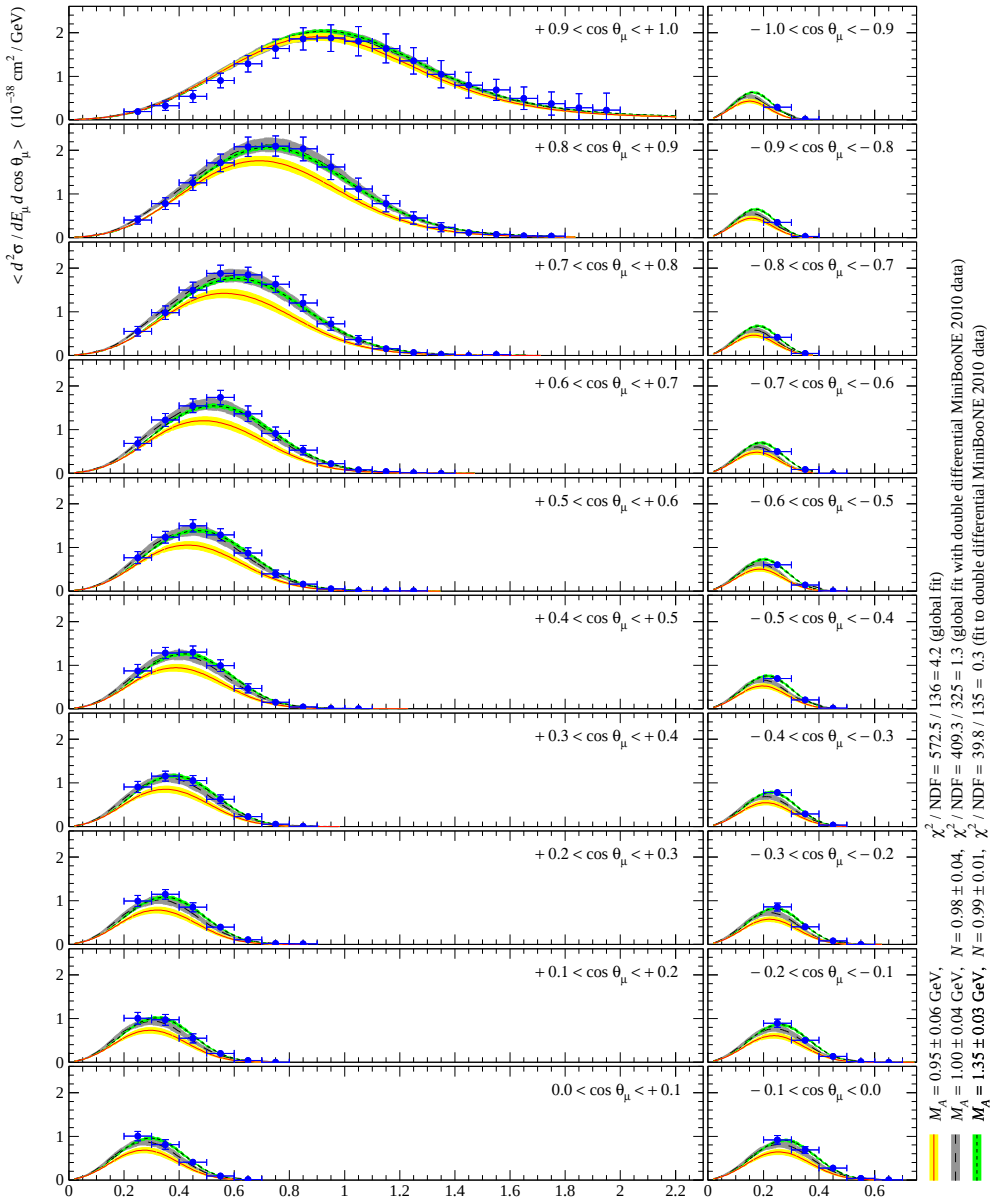

[1] Aguilar-Arevalo *et al.* (The MiniBooNE Collaboration), 2010.

[2] Martini, Ericson & Chanfray, 2011.

Effective (RFG) and constant M_A

We do not have properly working nuclear model for all energy ranges!

There is some dependence on E_ν in experimental values of M_A extracted with the RFG model.

So, we can fit experimental data to get $M_A^{\text{eff}}(E_\nu)$ using which will compensate nuclear effects.

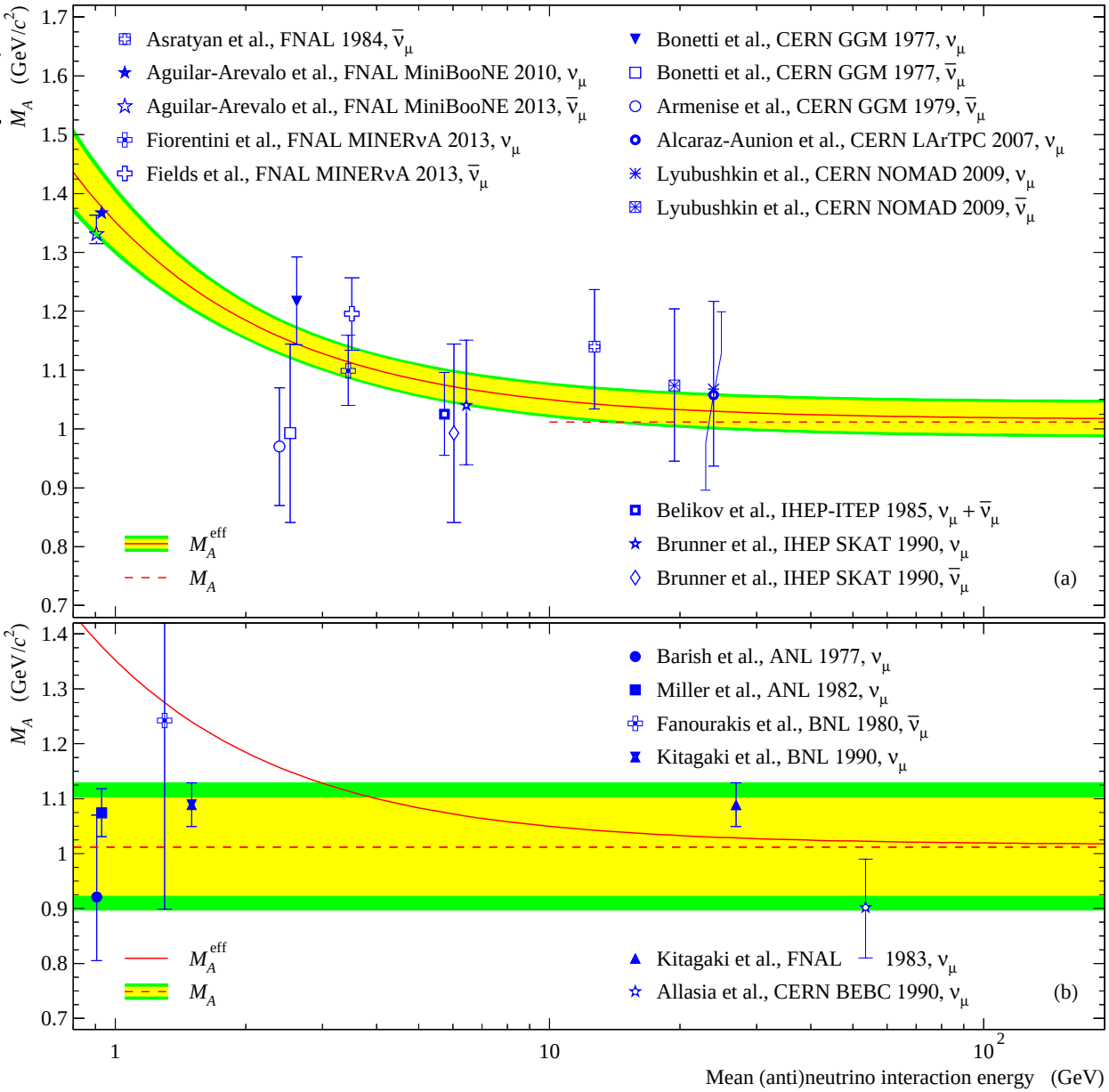

Effective (RFG) and constant M_A

$$M_A^{\text{eff}} = M_0 \left(1 + \frac{E_0}{E_\nu}\right),$$

$$M_0 = 1.015 \pm 0.026 \left(^{+0.032}_{-0.031}\right) \text{ GeV},$$

$$E_0 = 0.331 \left(^{+0.06}_{-0.056}\right) \left(^{+0.072}_{-0.066}\right) \text{ GeV}.$$

Total QES $\nu_\mu n$ & $\overline{\nu}_\mu p$ cross sections measured in experiments with deuterium, hydrogen & carbon/propane targets.[1]

[1] Kuzmin & Naumov, in preparation.

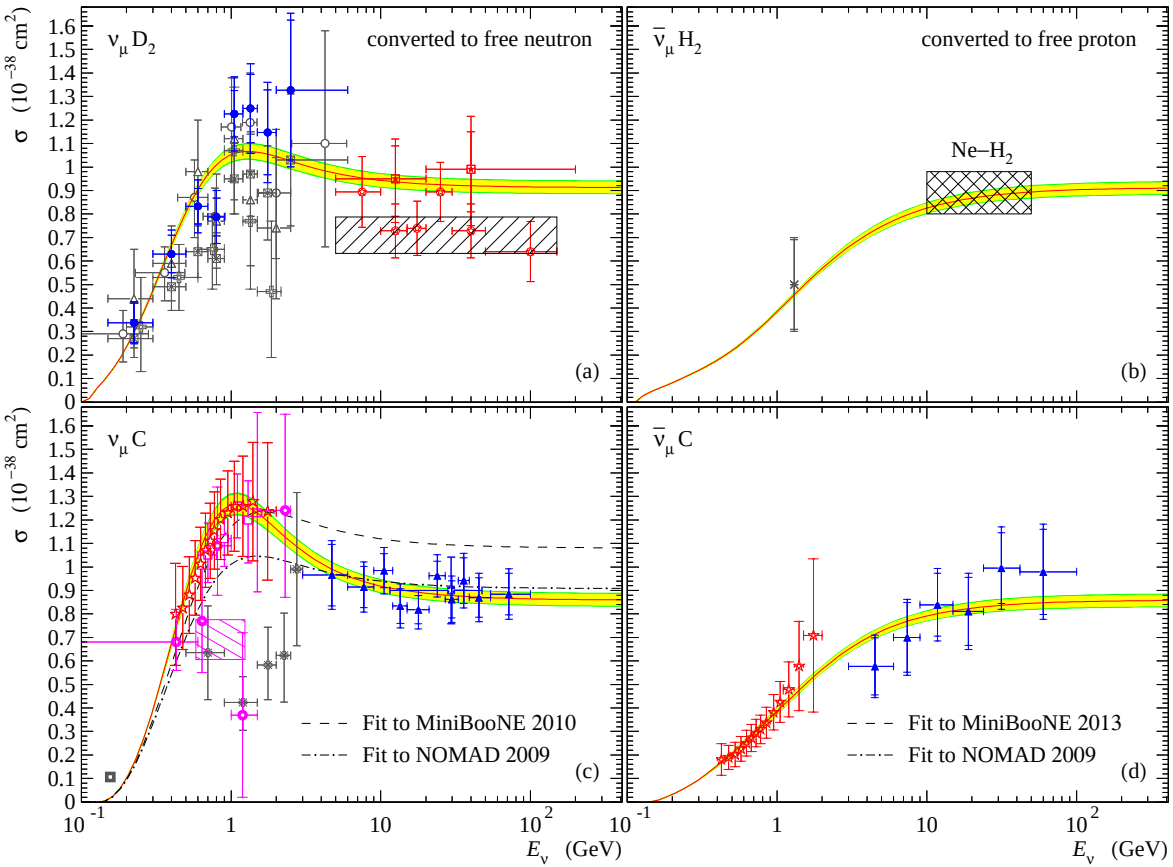

NOνA event topology

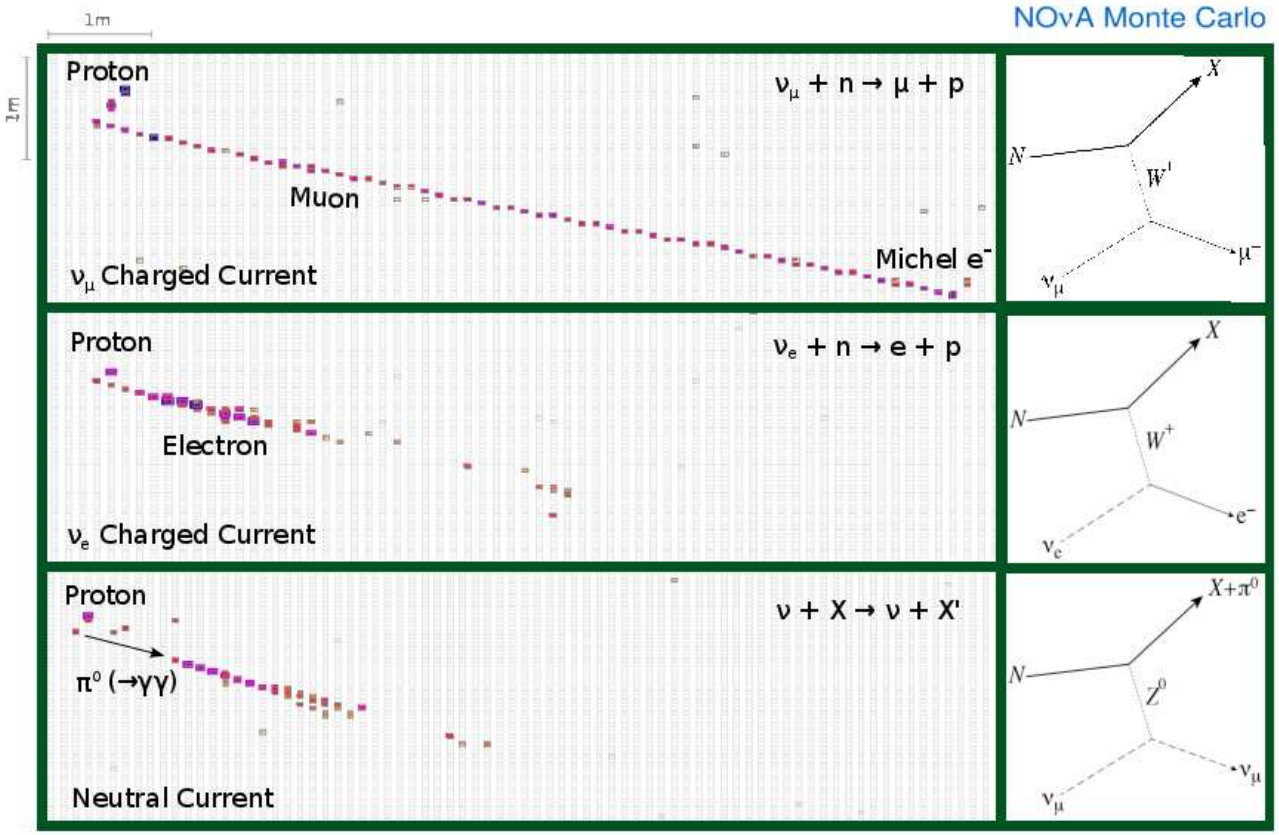

ν_μ CC

- long well-defined μ-track
- short p-track with large energy deposition at the end

ν_e CC

- single EM shower
- characteristic development of EM shower

NC with π^0 final state

- multiple displaced EM showers
- possible gaps near event vertex

QES event rates in the Near Detector of NOνA (ν mode)

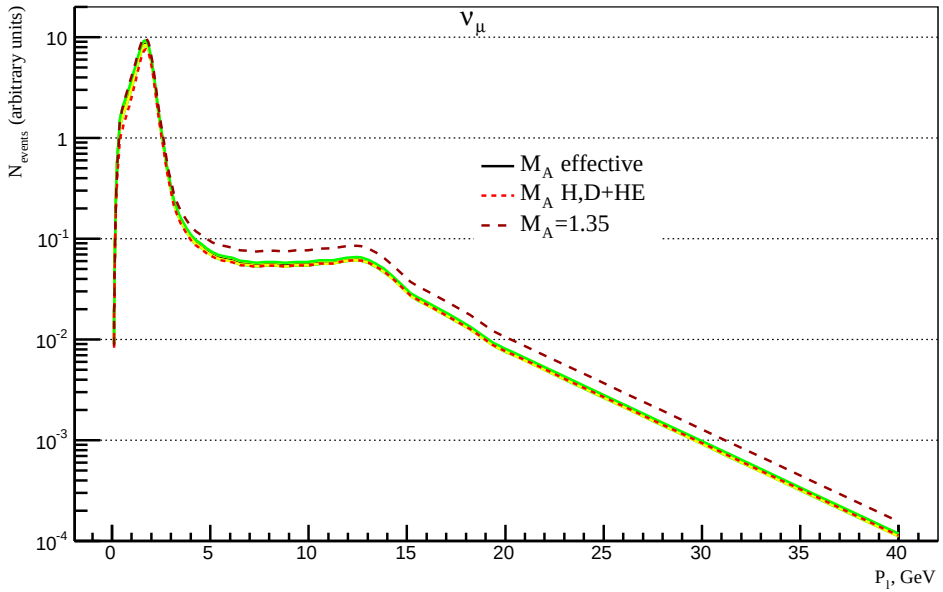

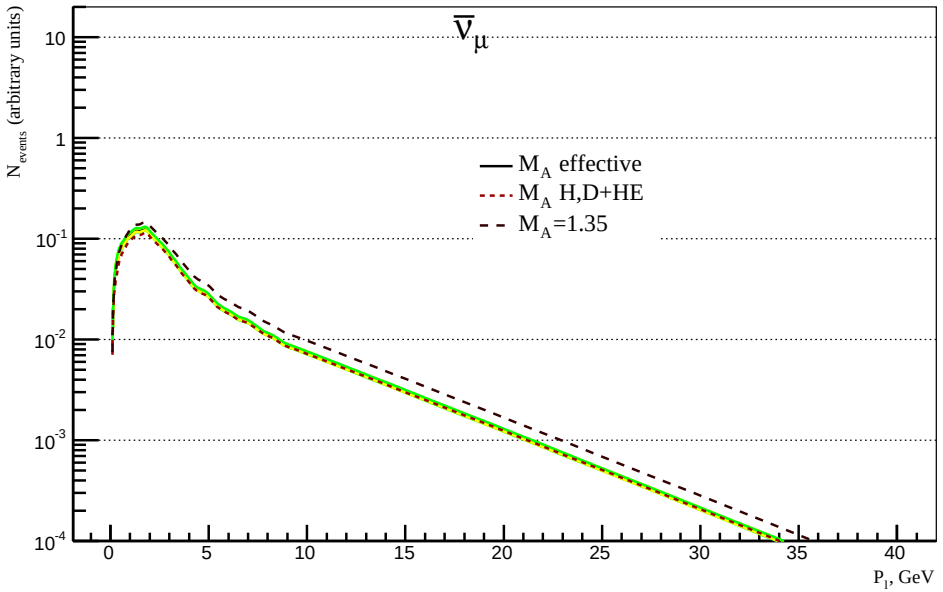

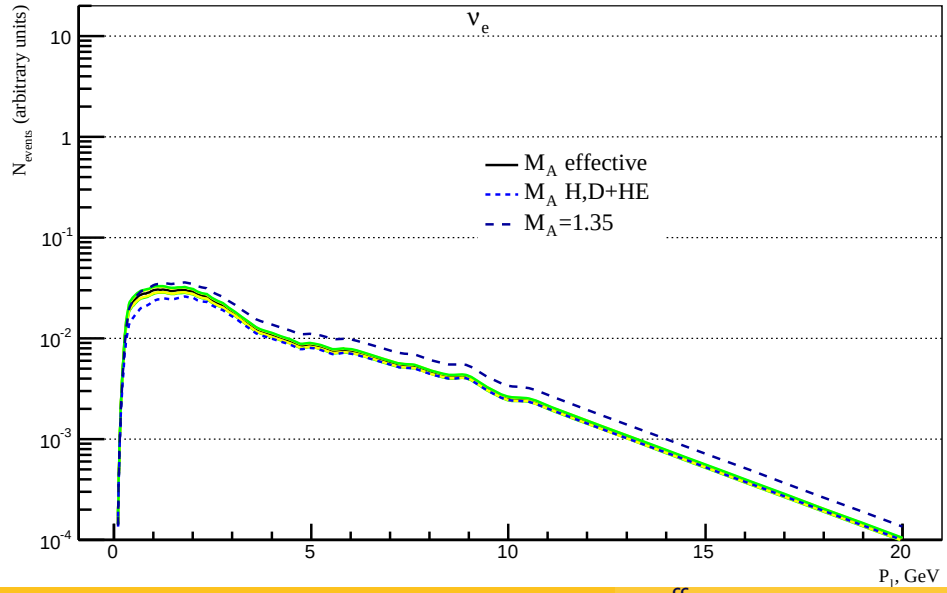

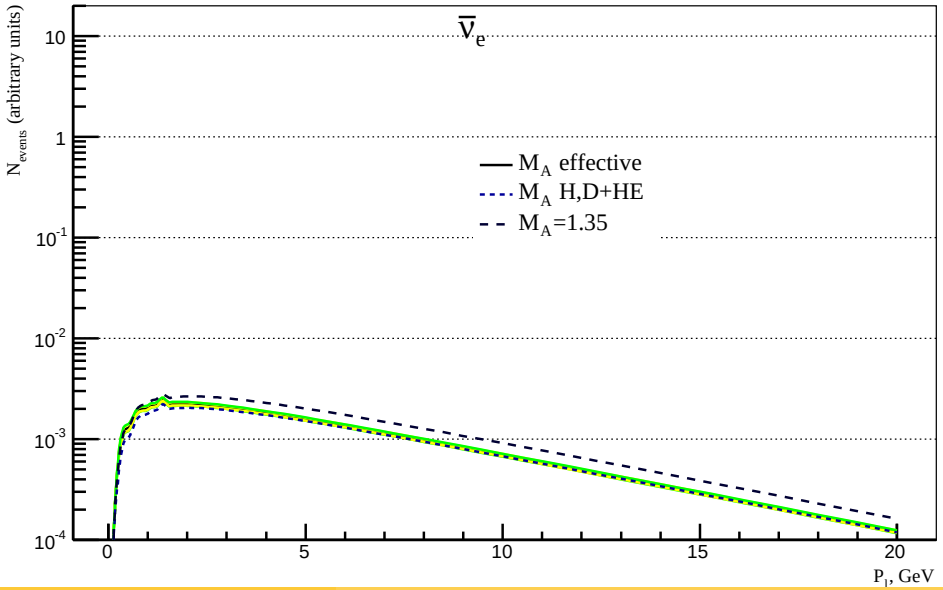

QES event rates in the Near Detector of NOνA (ν mode)

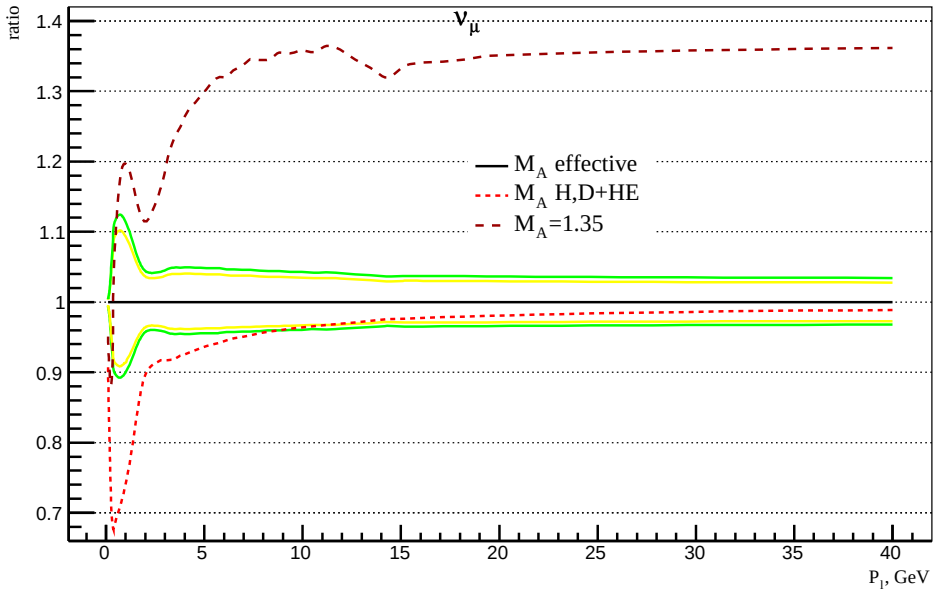

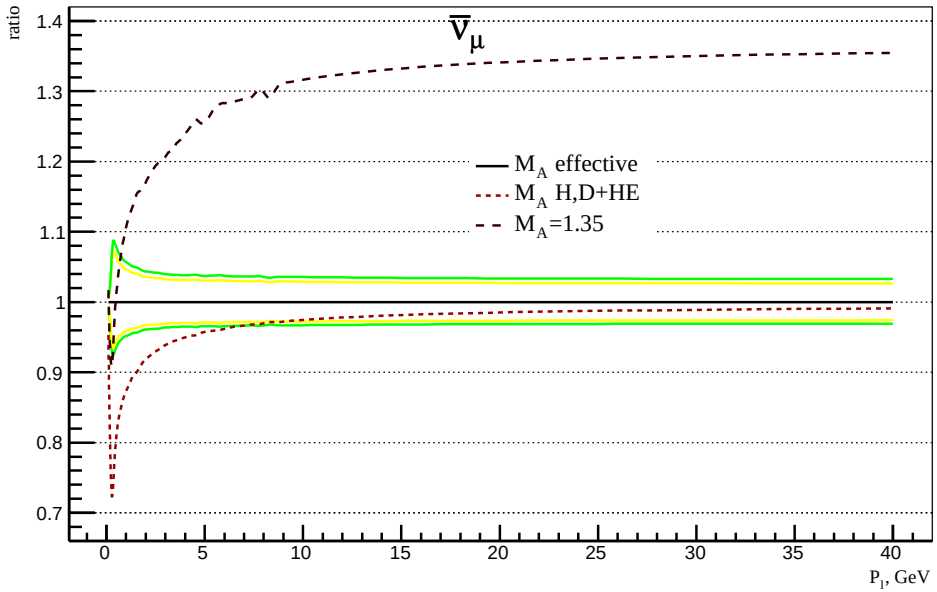

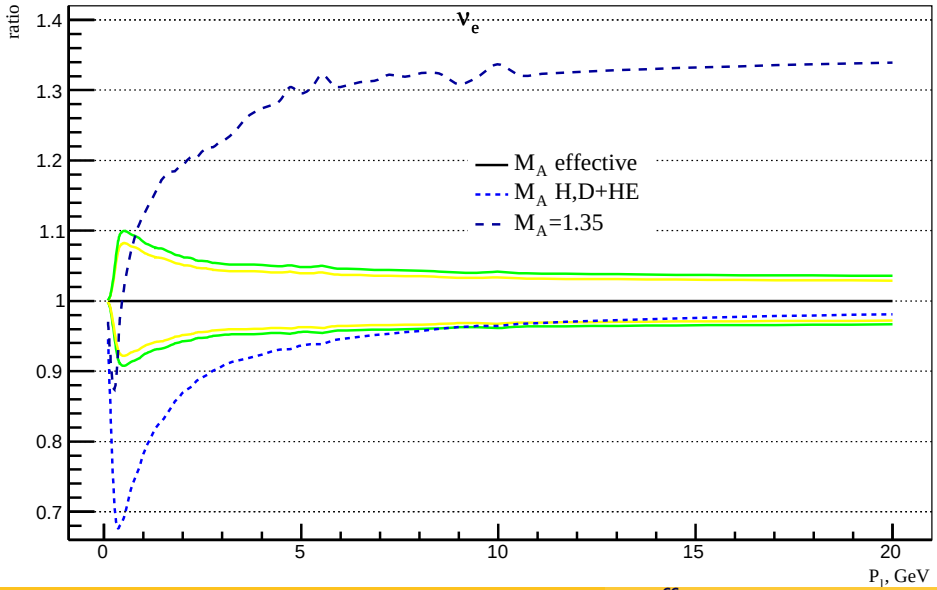

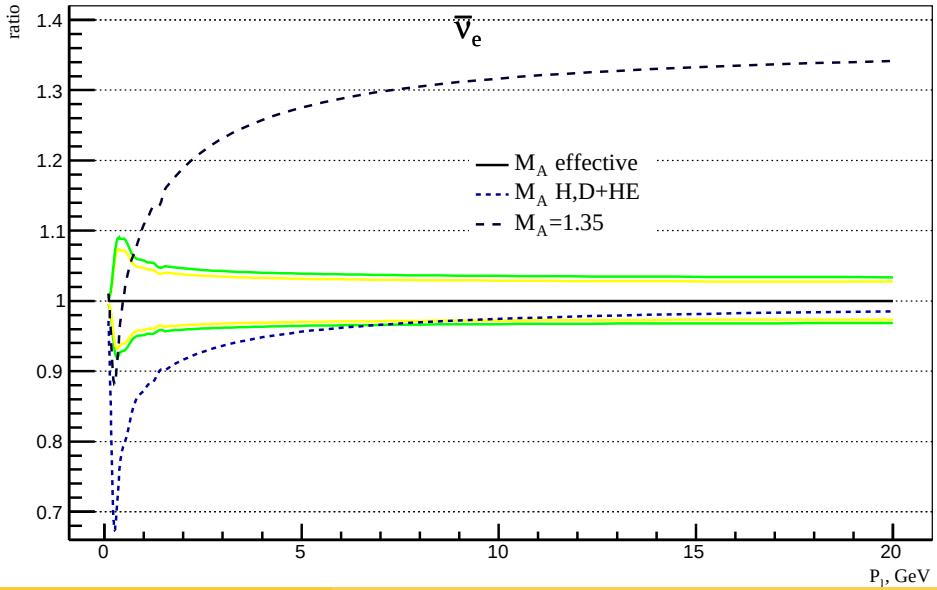

QES event rates in Super-Kamiokande

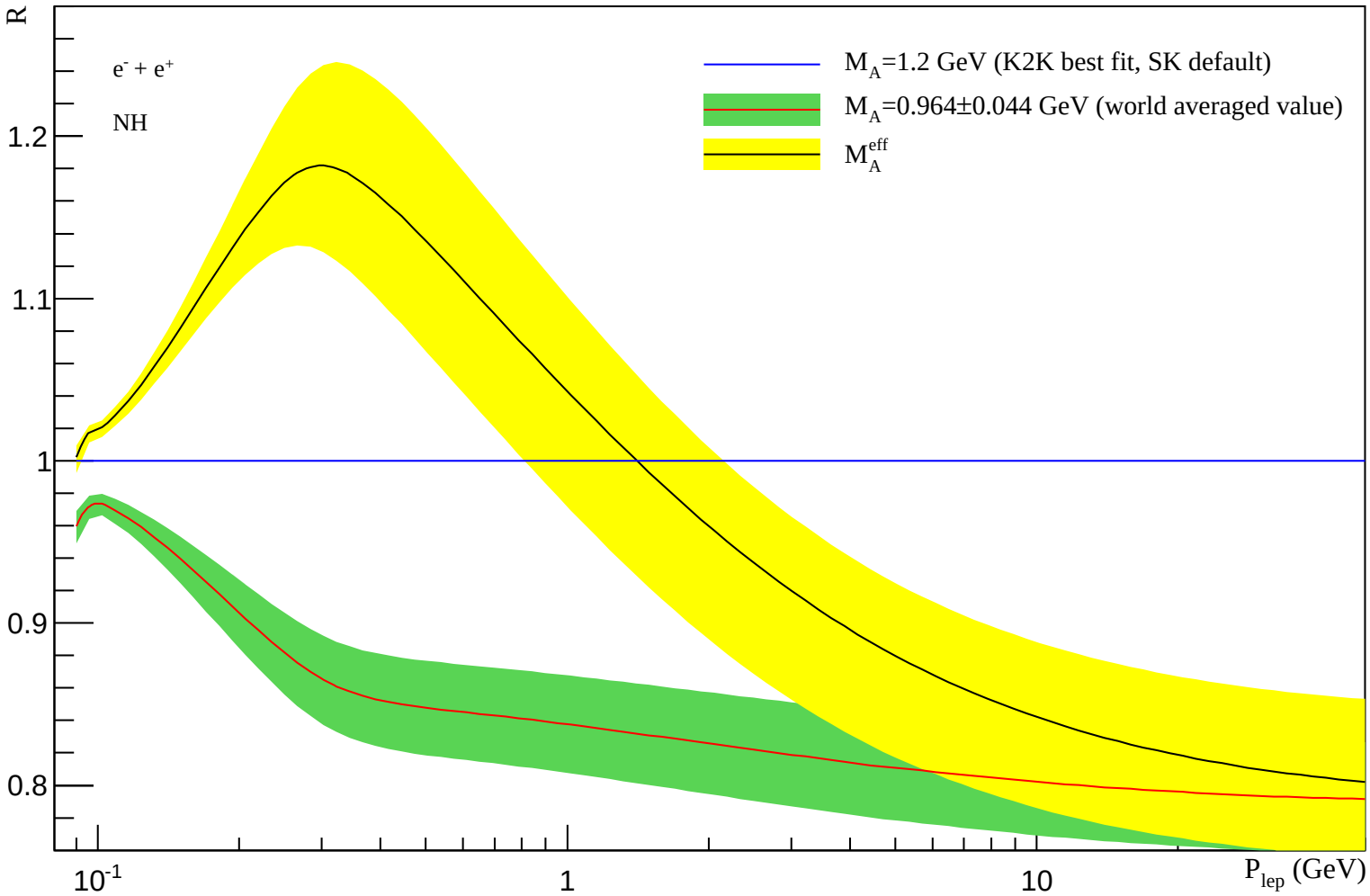

Electron QES event rates in the SK detector evaluated with several values of constant M_A and normalized to the rates calculated with the M_A^{eff}.

The calculations are done for NH.

QES event rates in Super-Kamiokande

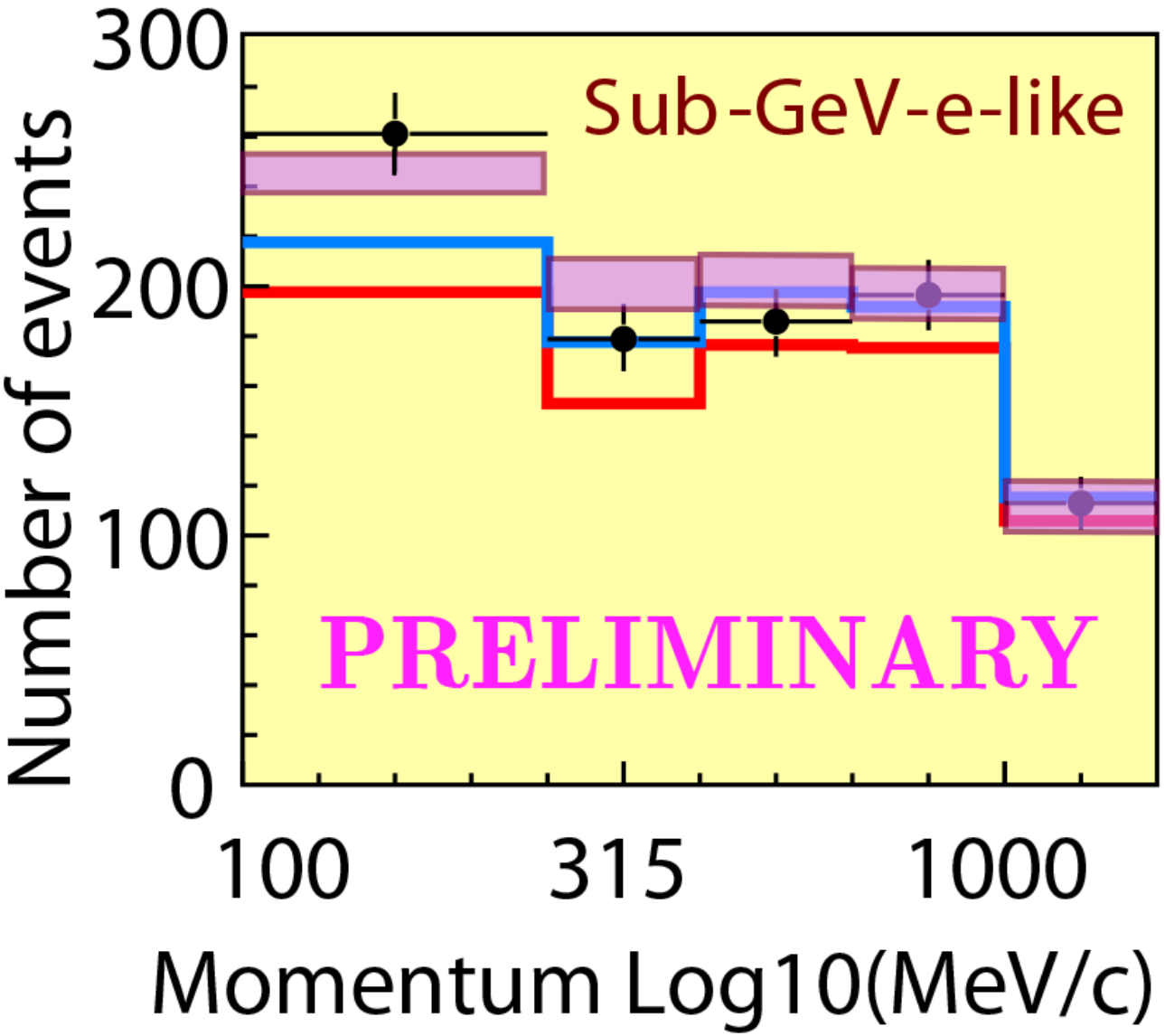

Conclusions

- The M_A value essentially affects the predicted count rates.
- The effect should be taken into account.
- Using the effective axial mass instead of the constant values like:
  - 1.35 GeV (MiniBooNE)[1] or 1.38 GeV (T2K)[2]
  - 1.05 GeV (NOMAD)[3]

  should improve the validity of the mixing parameter values.
- The estimations presented herein are preliminary.

[1] Aguilar-Arevalo *et al.* (The MiniBooNE Collaboration), 2010.
[2] Hadley (The T2K Collaboration), 2013.
[3] Lyubushkin (NOMAD Collaboration), 2009.

THANK YOU!

QES of neutrino on the nucleon

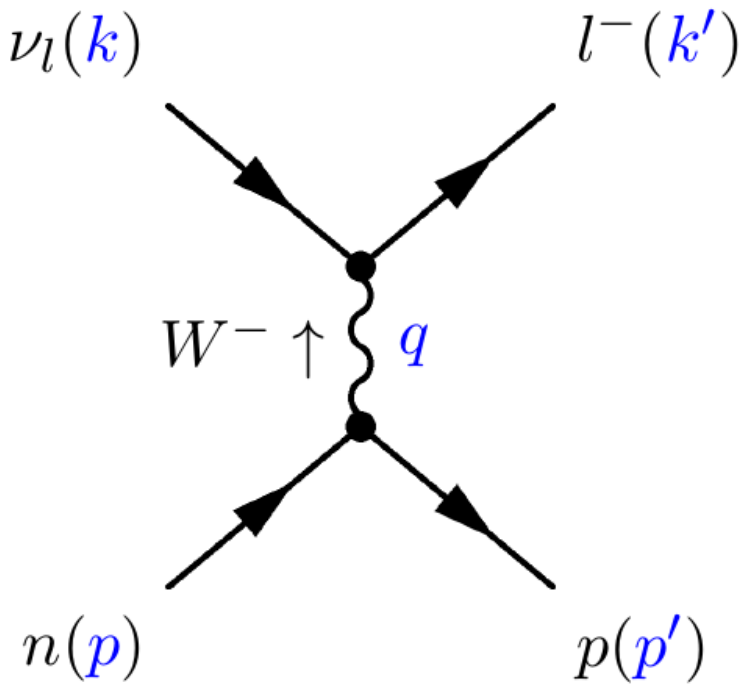

$$\nu_l + n \to l^- + p$$

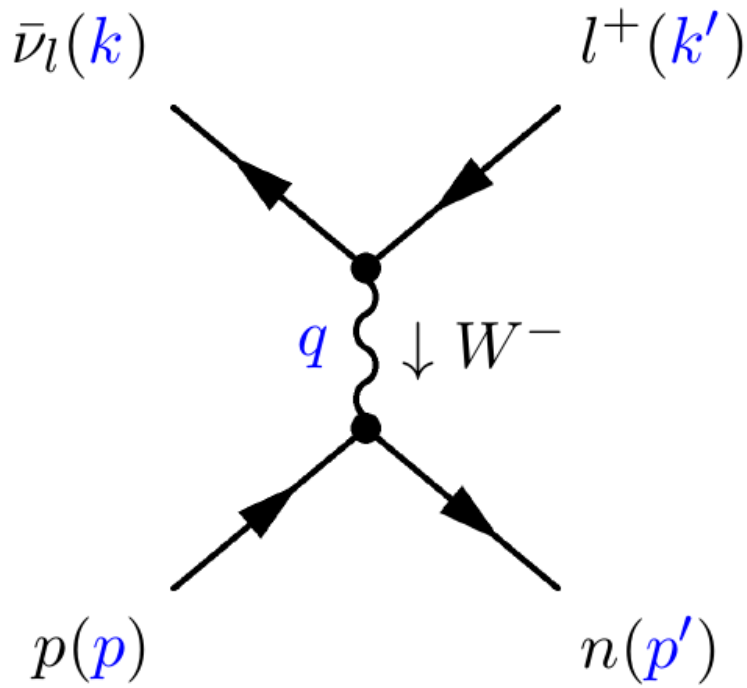

$$\bar{\nu}_l + p \to l^+ + n$$

$$Q^2 = -q^2$$

Electroweak form factors of the nucleon

$$\Gamma_\alpha(p,q) = \gamma_\alpha F_V + i\sigma_{\alpha\beta}\frac{q^\beta}{2M}F_M + \frac{q_\alpha}{M}F_S + \\ + \left(\gamma_\alpha F_A + \frac{p_\alpha + p'_\alpha}{M}F_T + \frac{q_\alpha}{M}F_P\right)\gamma_5.$$

C and T invariance of the hadron current $\Rightarrow$

$$\text{scalar } F_S = \text{tensor } F_T = 0.$$

Dirac and Pauli electromagnetic form factors:

$$F_V = \frac{G_E + x' G_M}{1 + x'}, \quad F_M = \frac{G_M - G_E}{1 + x'} \quad \text{where } x' = \frac{Q^2}{4M^2}.$$

Sachs form factors:

$$G_E = G_E^p - G_E^n, \quad G_M = G_M^p - G_M^n,$$

BBBA(2007) model is used for $G_E^{p,n}$ & $G_M^{p,n}$.

Martini *et al.* model

Martini *et al.* model incorporates relativistic corrections in the nuclear response functions and includes the multinucleon component of the "particle-hole" (2p-2h and 3p-3h contributions) processes. The model describes parameters of the "particle-hole" force which governs the collective aspect of the nuclear response via the random phase approximation. In the case of the MiniBooNE experiment multinucleon ejection is not distinguishable from single-nucleon production. The quasielastic cross section thus defined contains a certain proportion of 2p-2h and 3p-3h excitations. This proportion is large for neutrinos, which may be the interpretation of the increase in the axial cutoff mass needed to describe the data in the relativistic Fermi gas.[1]

[1] Martini, Ericson & Chanfray, 2011.

Neutrino oscillation theory

$$P_{\alpha\beta}(E_\nu, L) = \sum_{ij} V_{\alpha i} V_{\beta j} (V_{\alpha j} V_{\beta i})^* \exp\left(2\pi i \frac{L}{L_{ij}}\right)$$

$$L_{ij} = \frac{4\pi E_\nu}{\Delta m^2_{ij}}$$

$$V = O_{23} \Gamma_D O_{13} \Gamma_D^\dagger O_{12} \Gamma_M$$

$$\Gamma_D = \mathrm{diag}(1, 1, e^{i\delta}), \quad \Gamma_M = \mathrm{diag}(e^{i\phi_1}, e^{i\phi_2}, 1)$$

$$O_{12} = \begin{pmatrix} c_{12} & s_{12} & 0 \\ -s_{12} & c_{12} & 0 \\ 0 & 0 & 1 \end{pmatrix}, \quad O_{13} = \begin{pmatrix} c_{13} & 0 & s_{13} \\ 0 & 1 & 0 \\ -s_{13} & 0 & c_{13} \end{pmatrix}, \quad O_{23} = \begin{pmatrix} 1 & 0 & 0 \\ 0 & c_{23} & s_{23} \\ 0 & -s_{23} & c_{23} \end{pmatrix}$$

$$s_{ij} = \sin\theta_{ij}, \quad c_{ij} = \cos\theta_{ij}$$

RFG model

$$d\sigma^b = \frac{G_F^2 M_t}{16\pi^2 (kp)} \left(1 + \frac{Q^2}{M_W^2}\right)^{-2} L^{\alpha\beta} T_{\alpha\beta} \frac{d^3\vec{k}'}{2k'_0}$$

$$T_{\alpha\beta}(p_{\text{lab}}, q) = \int f(\vec{p}, \vec{q}) W_{\alpha\beta}(p, q) d\vec{p}$$

$$f(\vec{p}, \vec{q}) = {v_{\text{rel}}}^{-1} \bar{n}_i(\vec{p})[1 - n_f(\vec{p'})]$$

$$v_{\text{rel}} = \frac{(kp)}{M_t E_\nu}$$

Event rates

Flux of leptons l generated by QES of neutrino on one atom of ${}^{Z}_{A}\mathrm{El}$ per second:

$$\frac{dN_l^{\mathrm{El}}}{dp_l} = \begin{cases} \int \dfrac{d\sigma_{\bar{\nu}_l}}{dp_l}\bar{\nu}_l(E_\nu)dE_\nu, & \text{if } \mathrm{El} = \mathrm{H}; \\ \int \left(Z\dfrac{d\sigma_{\nu_l}^{\mathrm{El}}}{dp_l}\nu_l(E_\nu) + (A-Z)\dfrac{d\sigma_{\bar{\nu}_l}^{\mathrm{El}}}{dp_l}\bar{\nu}_l(E_\nu) \right) dE_\nu, & \text{if } \mathrm{El} \neq \mathrm{H}, \end{cases}$$

on one gramm $\mathrm{El}^1_{n_1}\mathrm{El}^2_{n_2}\ldots\mathrm{El}^m_{n_m}$ per second:

$$\frac{dN_l}{dp_l} = \frac{N_A}{\mu}\sum n_k \frac{dN_l^{\mathrm{El}^k}}{dp_l}.$$

QES cross section analysis

QES of $\nu_\mu n$ & $\overline{\nu}_\mu p$ on aluminium, iron/steel & freon targets.

The gray points are excluded from the global fit being either superseded by newer experiments, or not satisfying selection criteria.[1]

[1] Kuzmin & Naumov, in preparation.

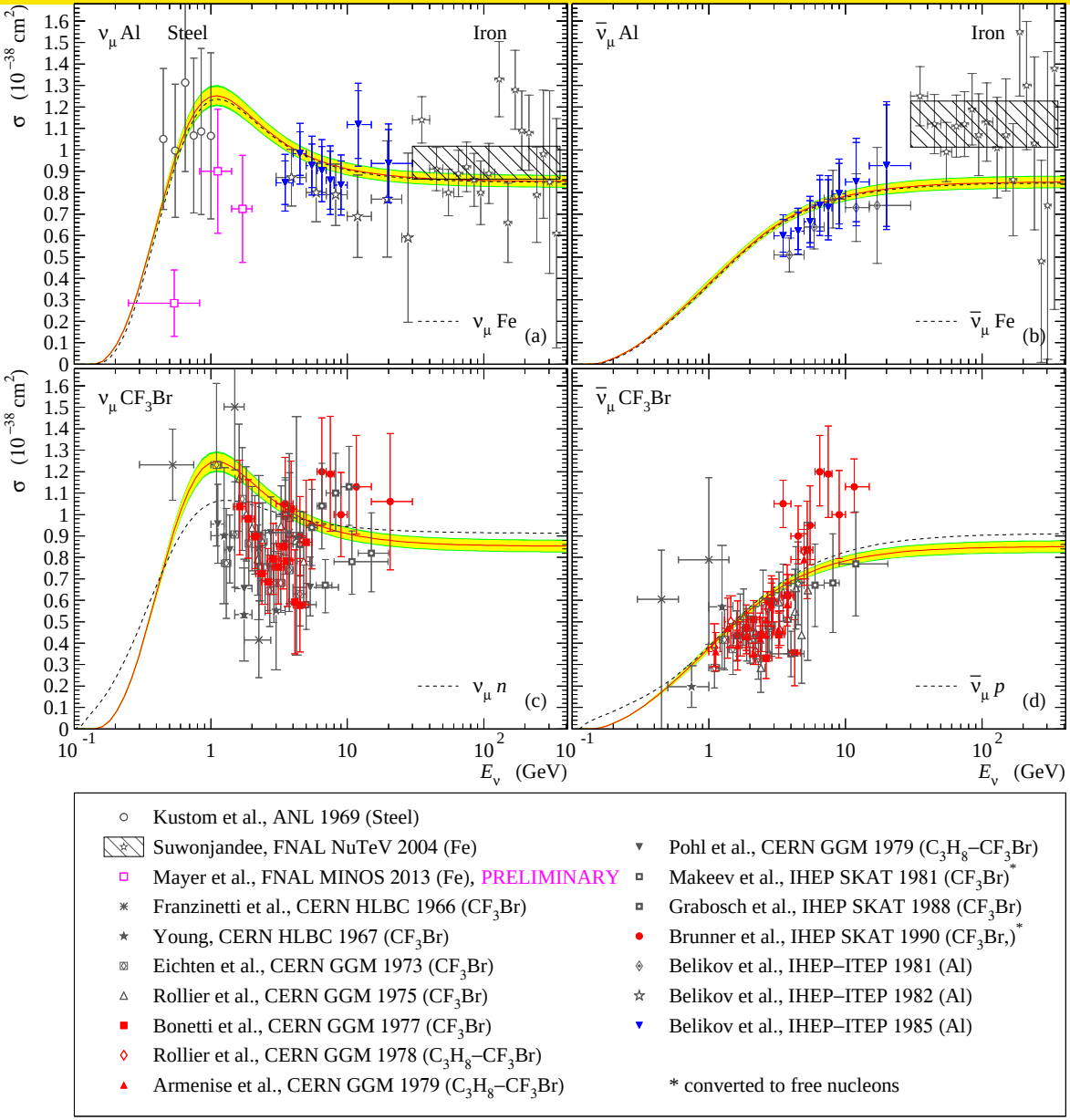

MiniBooNE ν

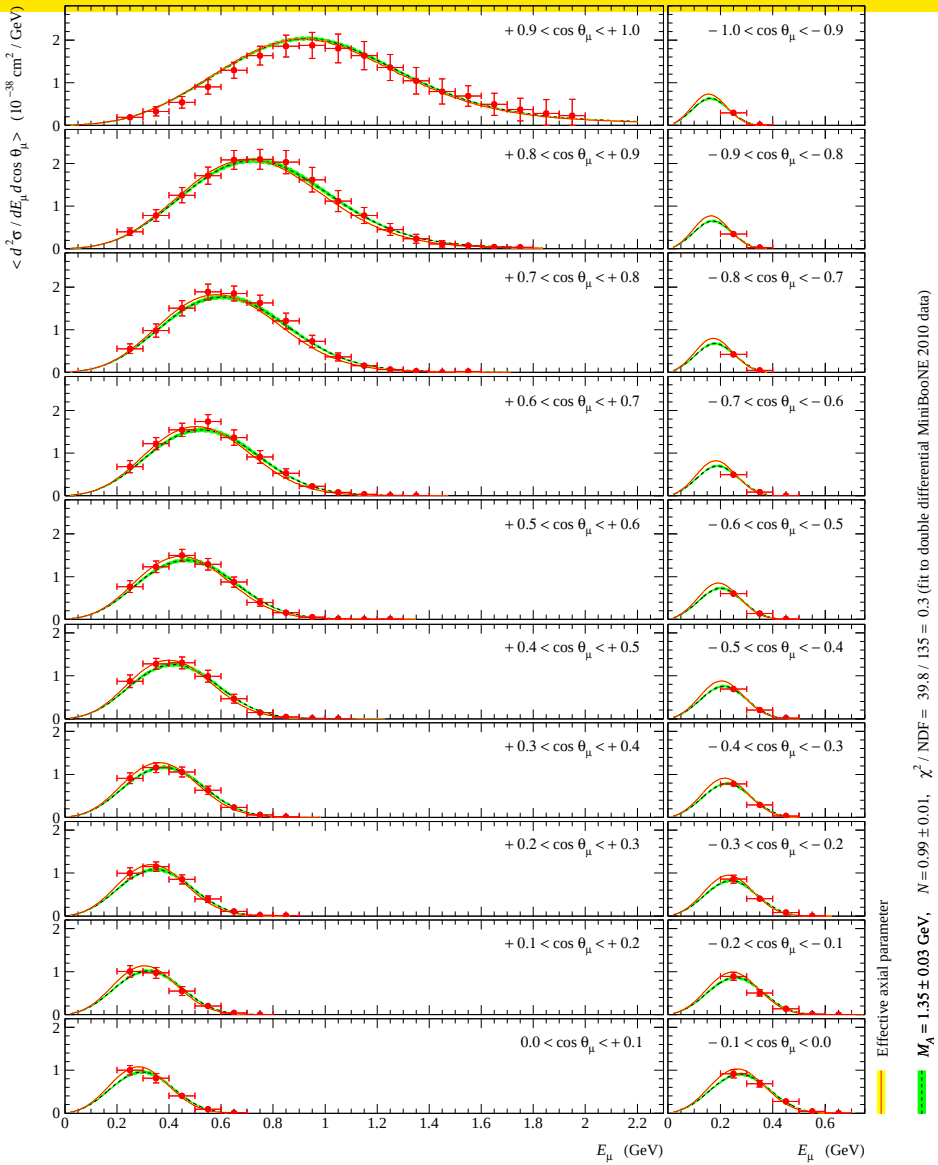

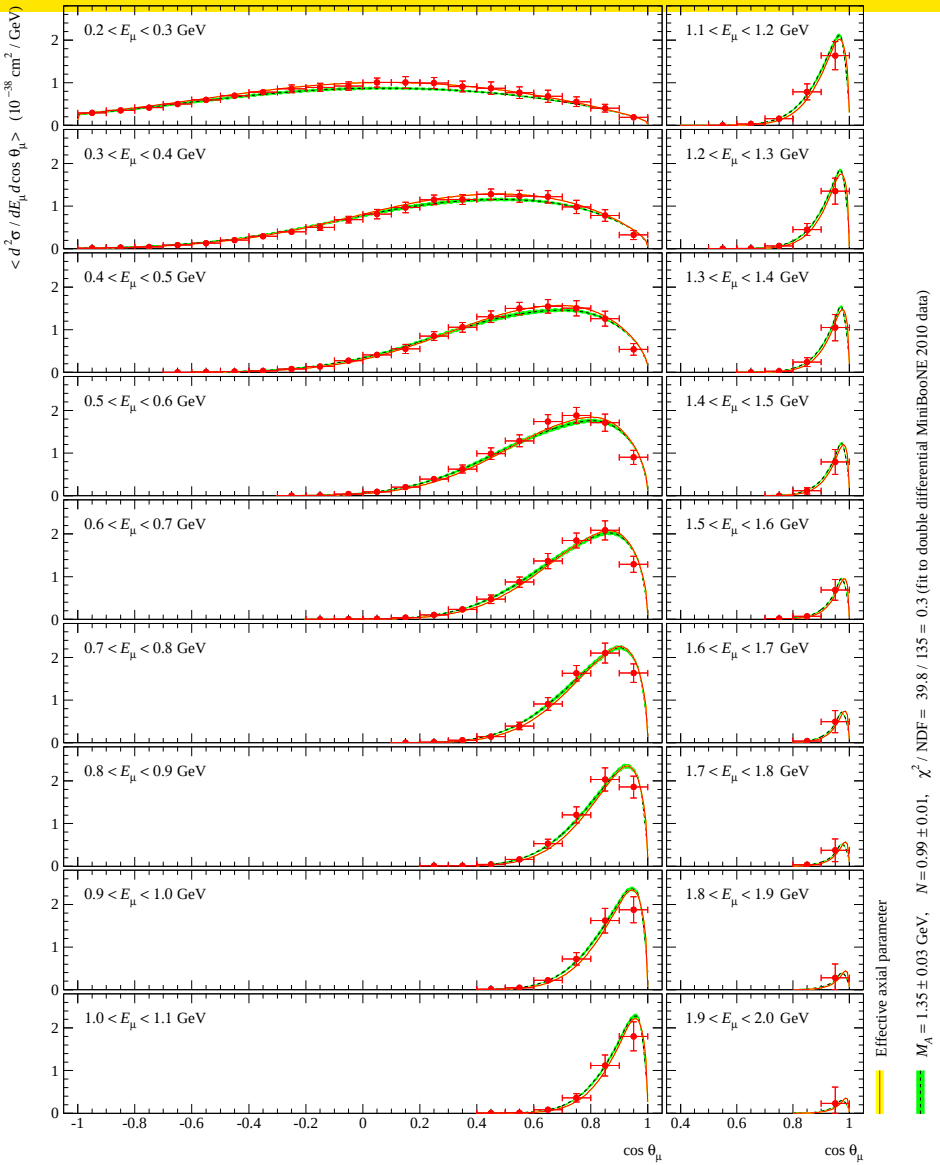

The red curves with the yellow bands are calculated by using M_A^{eff}.

MiniBooNE $\bar{\nu}$

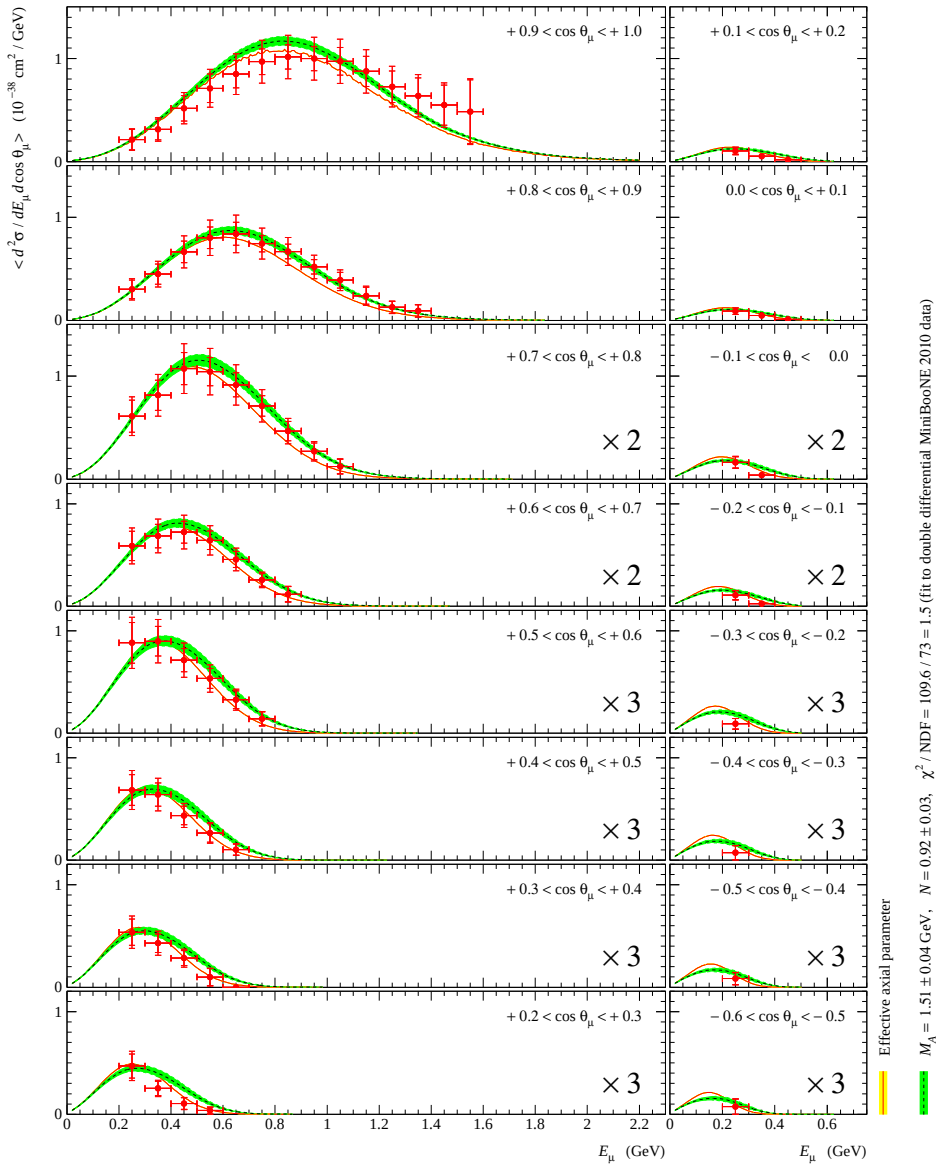

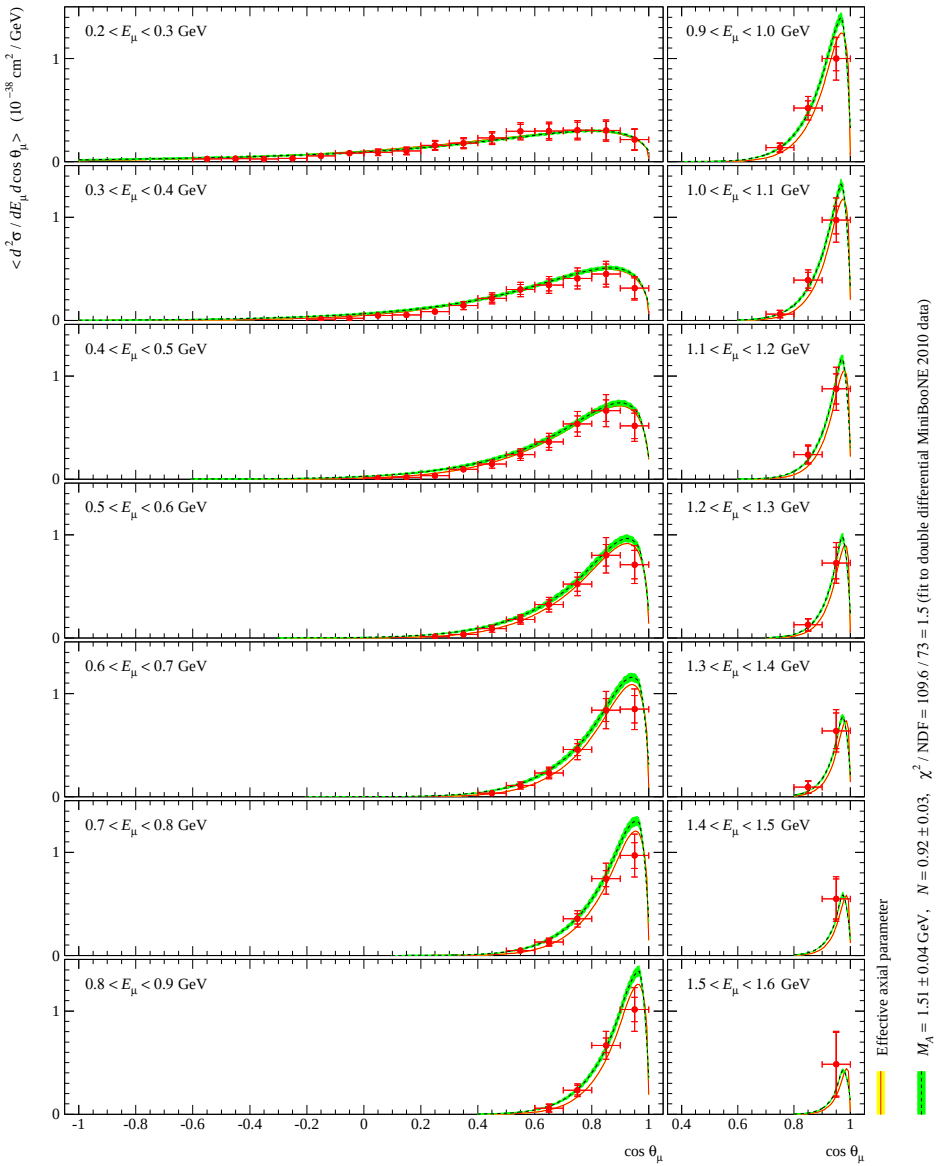

QES cross section in Minerva

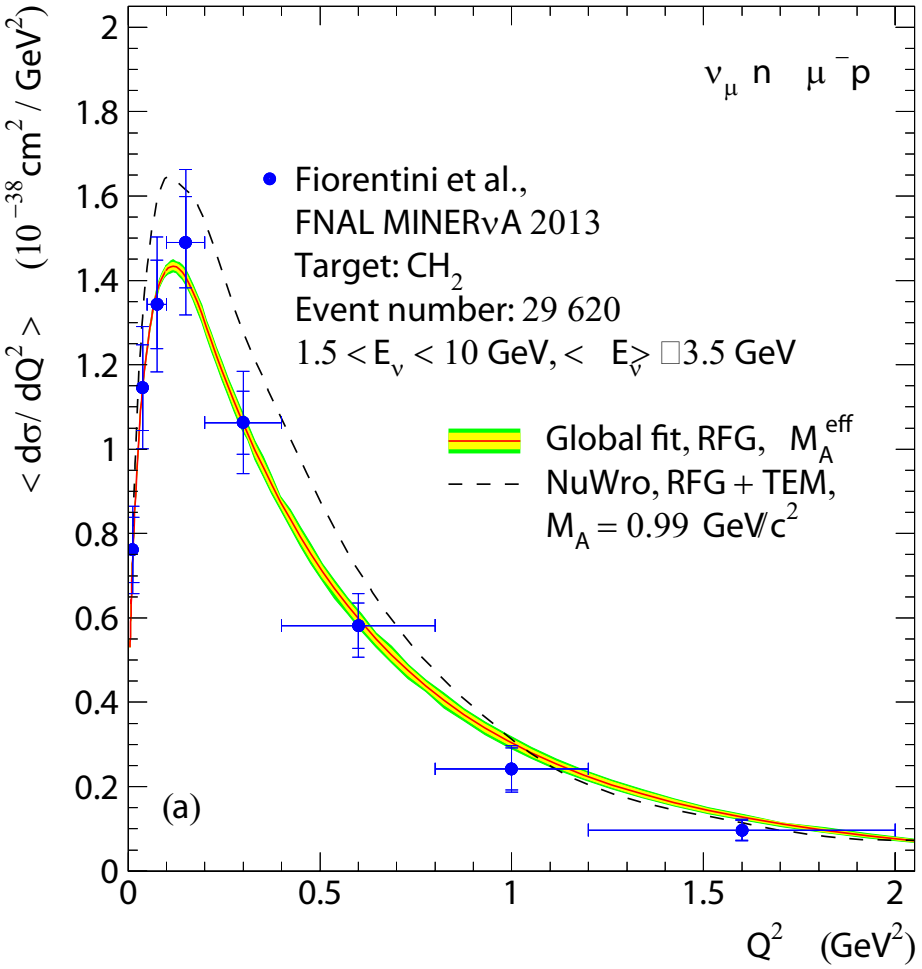

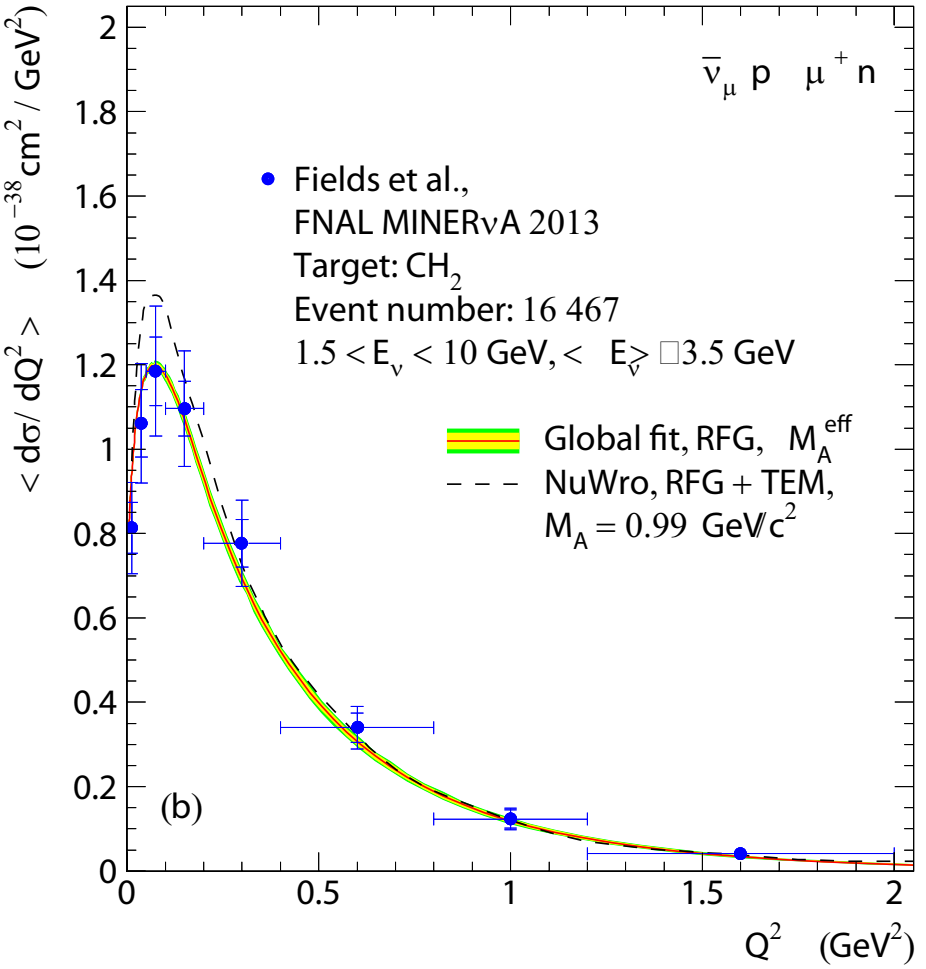

QES cross section in T2K

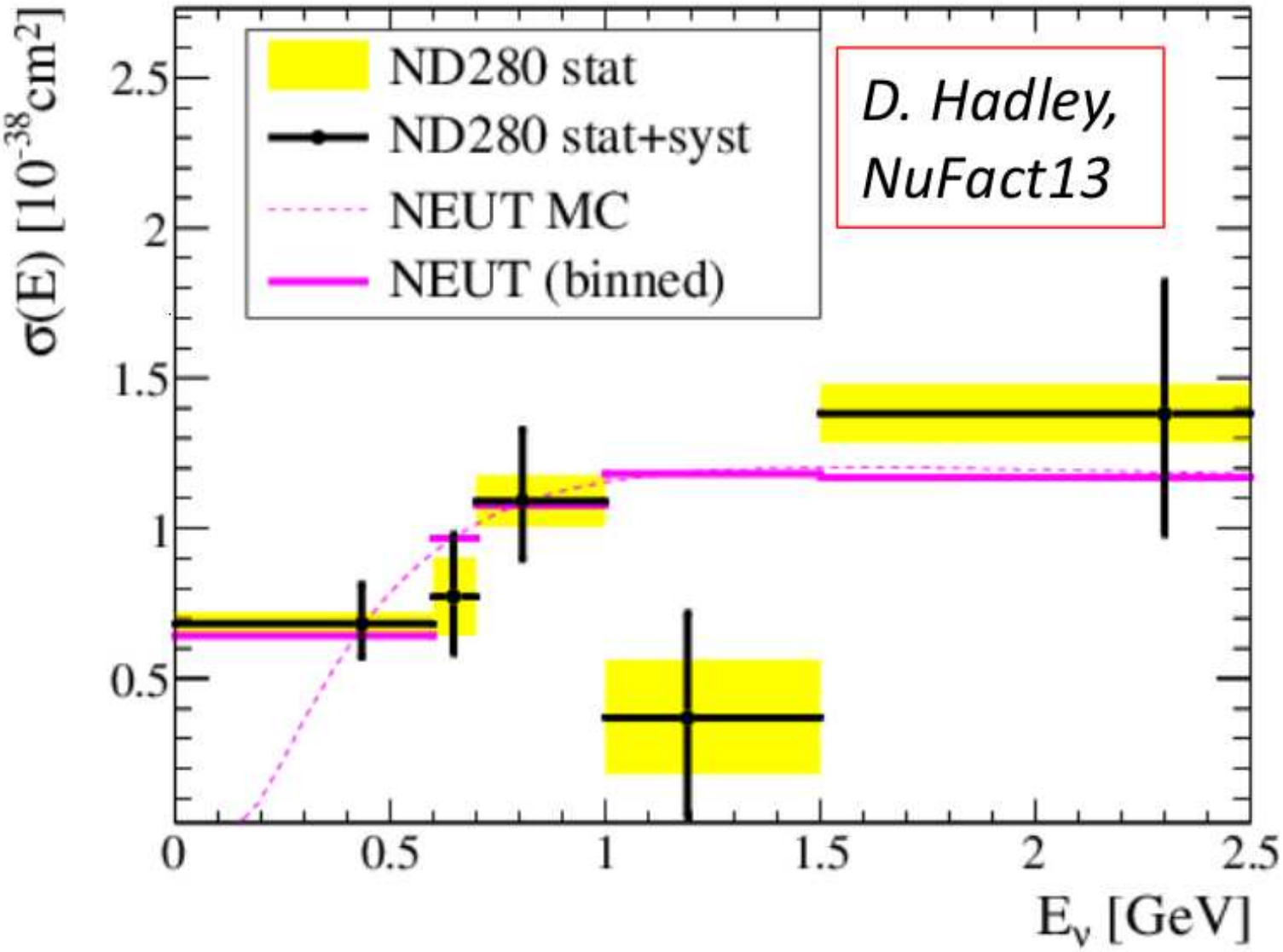

Fluxes in NOνA

ND:

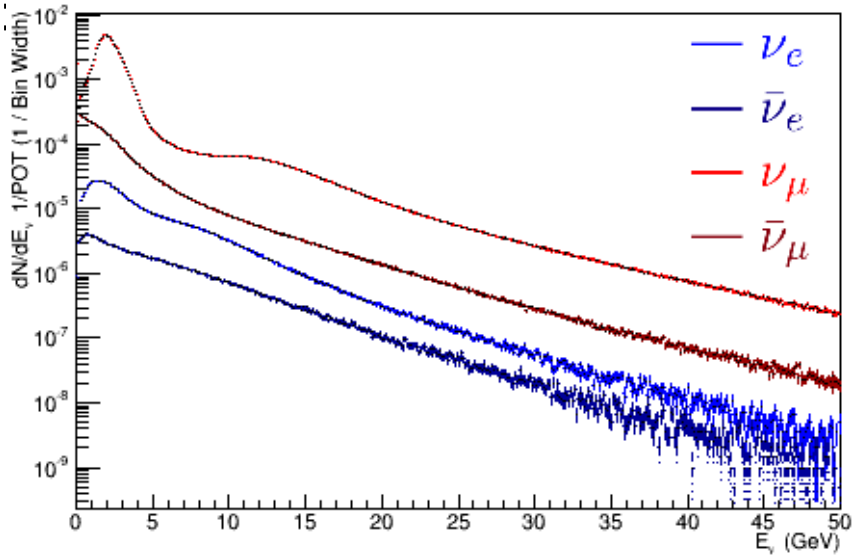

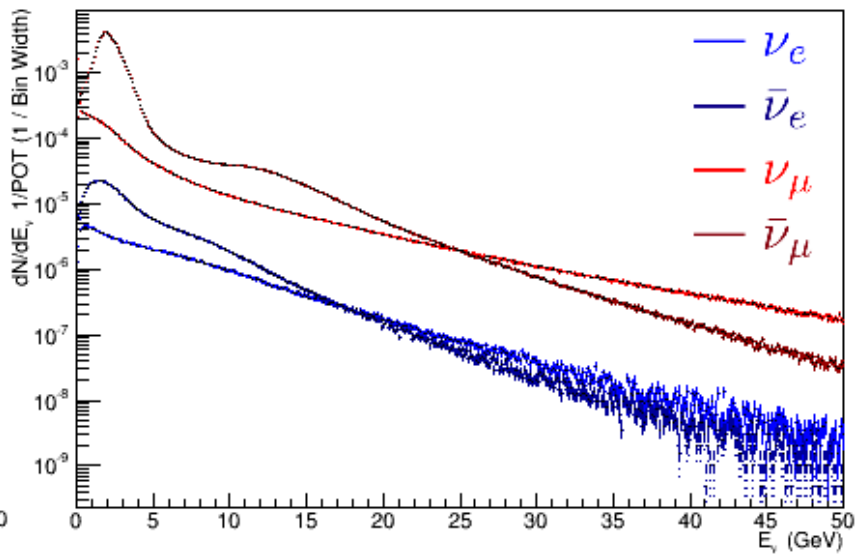

FD:

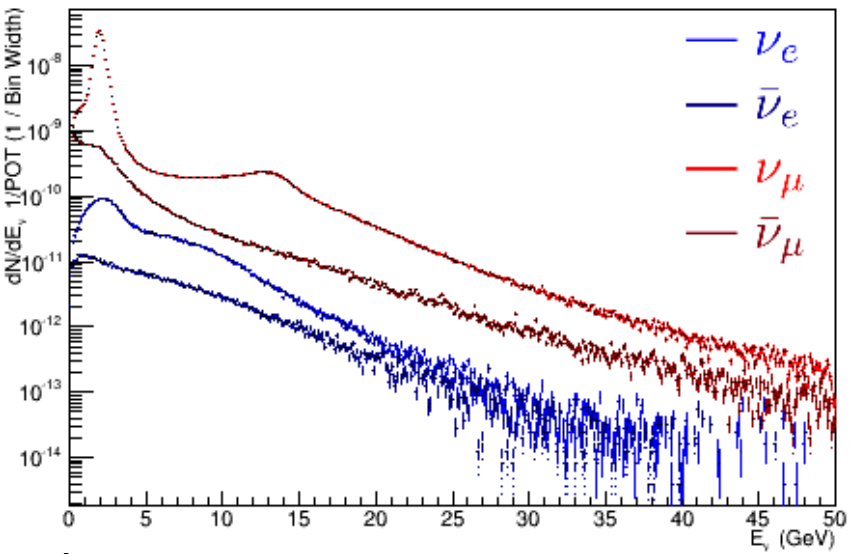

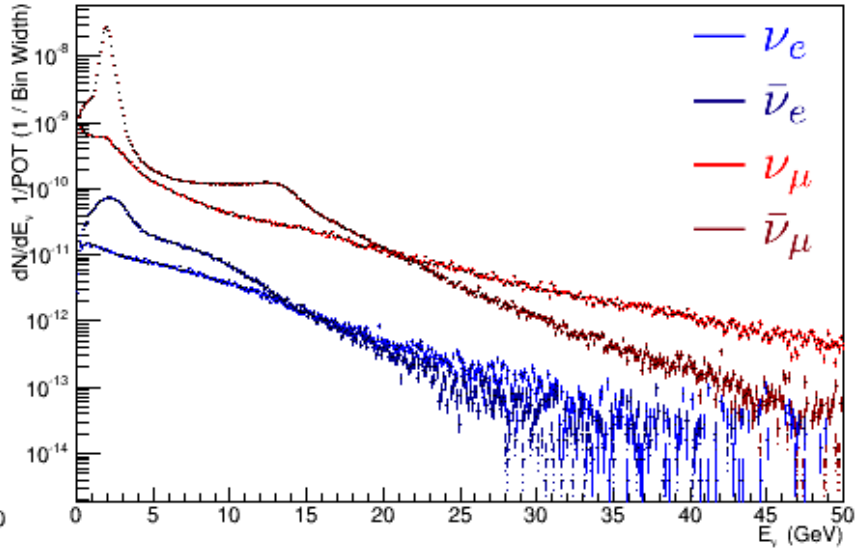

ν mode $\bar{\nu}$ mode

ν_μCC in NOνA

ν mode:

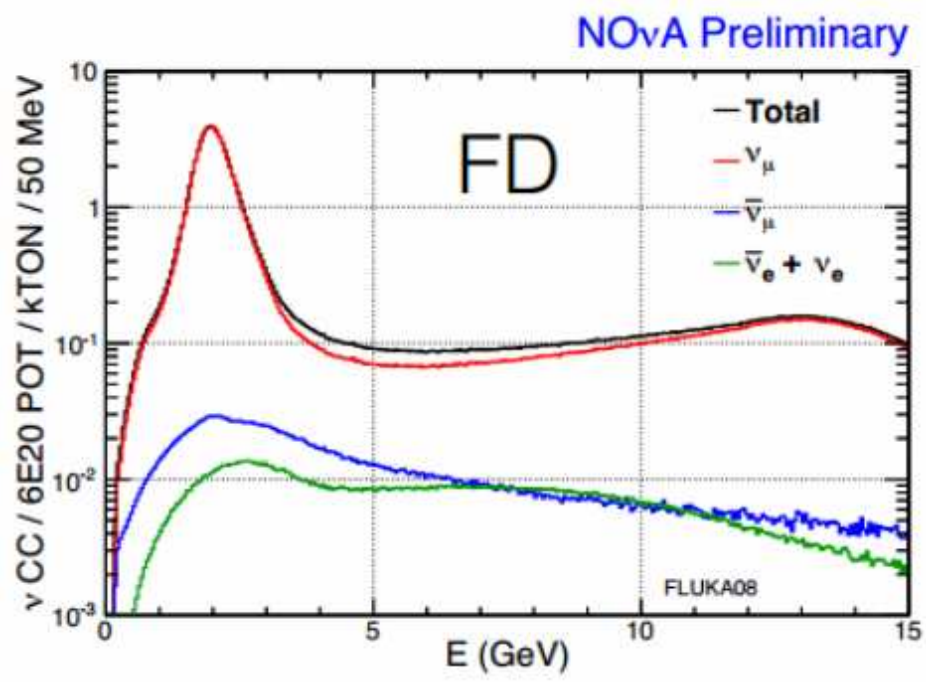

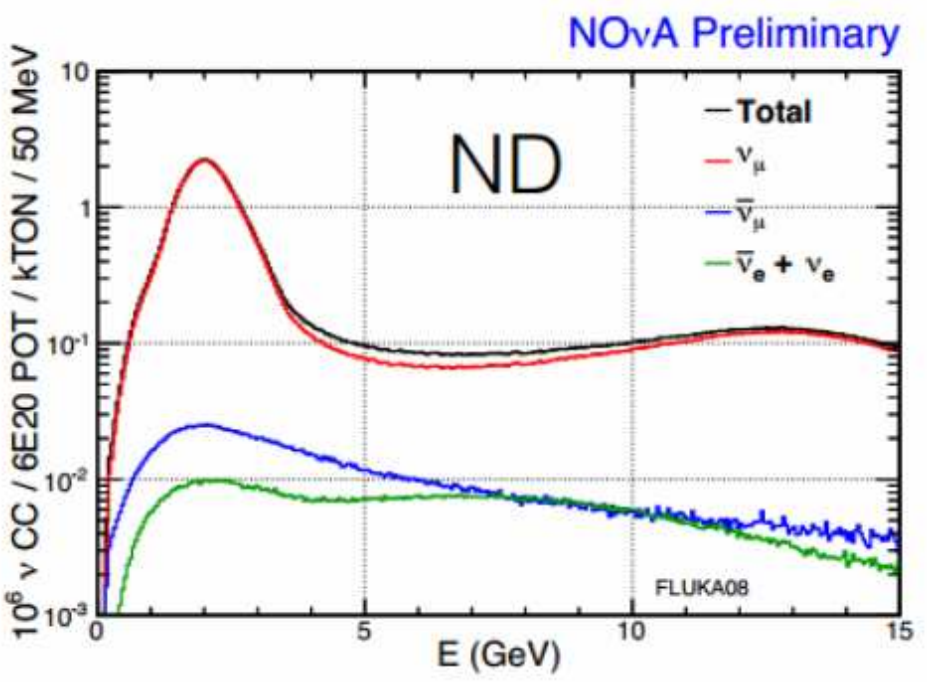

	[1,3]GeV	[0,120]Gev
Total	63.5	103.8
Numu	62.1	97.6
Anti-Numu	1.0	3.9
Nue+Anti-Nue	0.4	2.3

x10^6	[1,3]GeV	[0,120]Gev
Total	53.9	95.0
Numu	52.6	89.5
Anti-Numu	0.9	3.5
Nue+Anti-Nue	0.4	2.0

$\bar{\nu}_\mu$CC in NOνA

$\bar{\nu}$ mode:

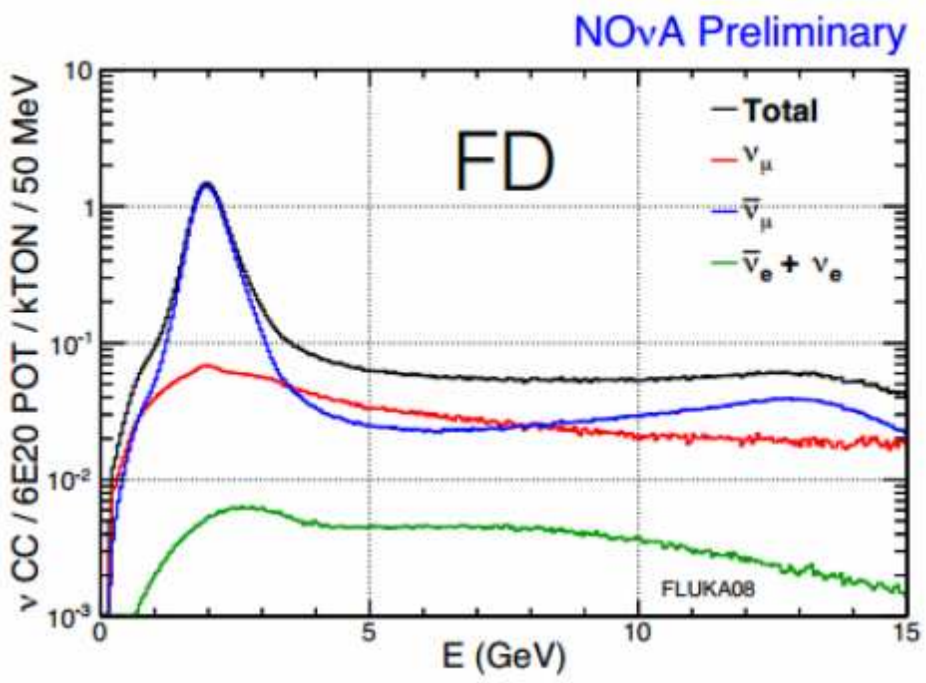

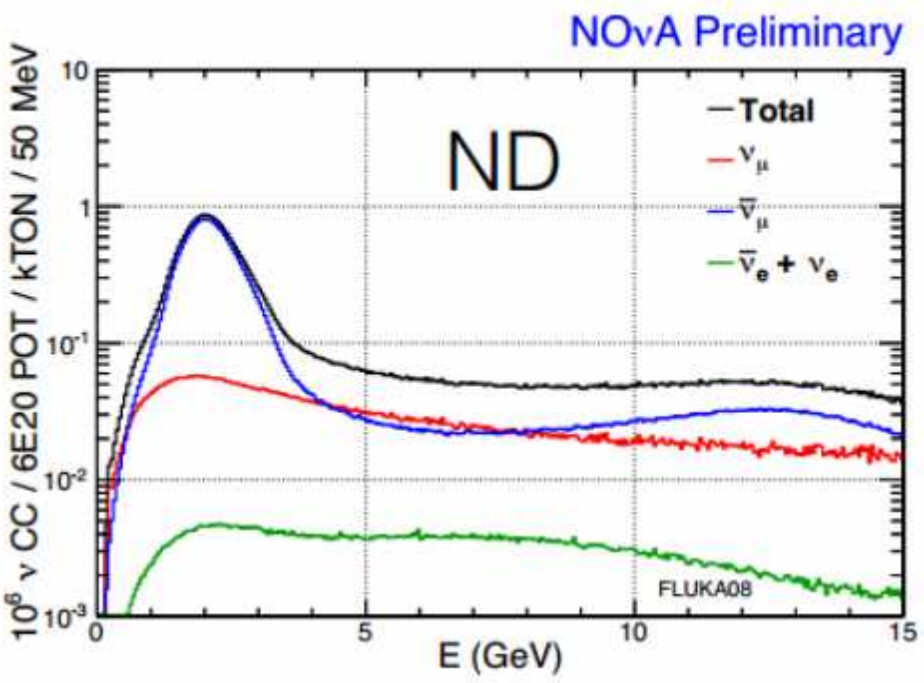

	[1,3]GeV	[0,120]Gev
Total	25.1	46.7
Numu	2.4	13.2
Anti-Numu	22.5	32.2
Nue+Anti-Nue	0.2	1.3

x10^6	[1,3]GeV	[0,120]Gev
Total	21.4	42.3
Numu	2.1	11.9
Anti-Numu	19.1	29.3
Nue+Anti-Nue	0.2	1.1

Atmospheric neutrino spectra

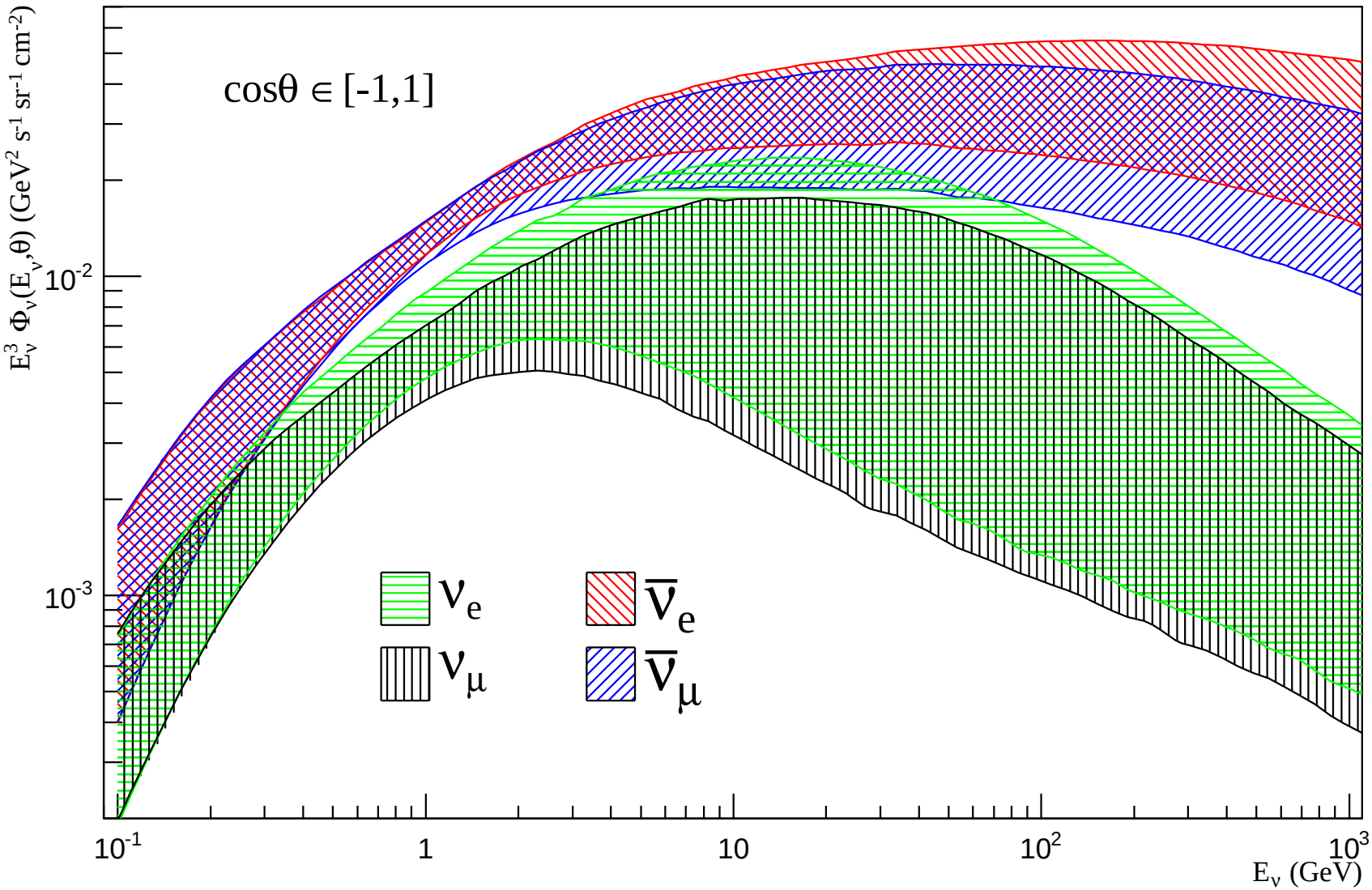

Atmospheric neutrino energy spectra at the Kamioka site by Honda et al.[1]

[1] Honda et al., 2011.

Density profile in the Earth

PREM: the Preliminary Reference Earth Model[1].

The Wolfenstein equations for the Earth density profile are solved[2].

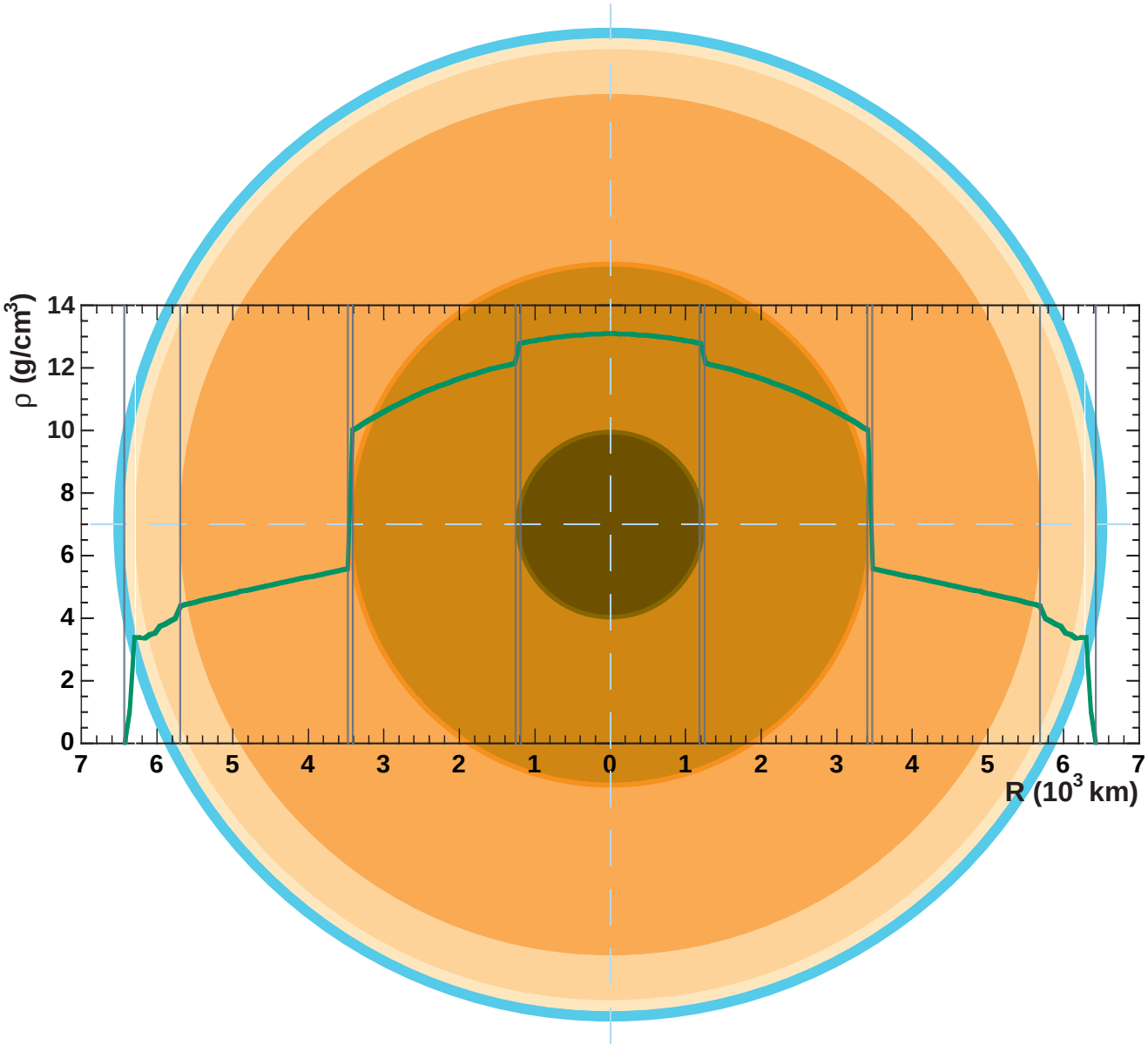

[1] Dziewonski & Anderson, 1981.

[2] Naumov, 1992.

Neutrino oscillation parameters

Table: Neutrino oscillation parameters for normal and inverse mass hierarchy[1]

parameter	best fit	1σ	2σ	3σ
Δm^2_{21} $[10^{-5}\text{eV}^2]$	7.62	$7.43 - 7.81$	$7.27 - 8.01$	$7.12 - 8.20$
$\lvert\Delta m^2_{31}\rvert$ $[10^{-3}\text{eV}^2]$	2.55 2.43	$2.46 - 2.61$ $2.37 - 2.50$	$2.38 - 2.68$ $2.29 - 2.58$	$2.31 - 2.74$ $2.21 - 2.64$
$\sin^2\theta_{12}$	0.320	$0.303 - 0.336$	$0.29 - 0.35$	$0.27 - 0.37$
$\sin^2\theta_{23}$	0.613 0.600	$0.400 - 0.461$ $0.573 - 0.635$ $0.569 - 0.626$	$0.38 - 0.66$ $0.39 - 0.65$	$0.36 - 0.68$ $0.37 - 0.67$
$\sin^2\theta_{13}$	0.0246 0.0250	$0.0218 - 0.0275$ $0.0223 - 0.0276$	$0.019 - 0.030$ $0.020 - 0.030$	$0.017 - 0.033$
δ	0.80π -0.03π	$0 - 2\pi$	$0 - 2\pi$	$0 - 2\pi$

[1] Forero, Tortola & Valle, 2012.

Oscillograms

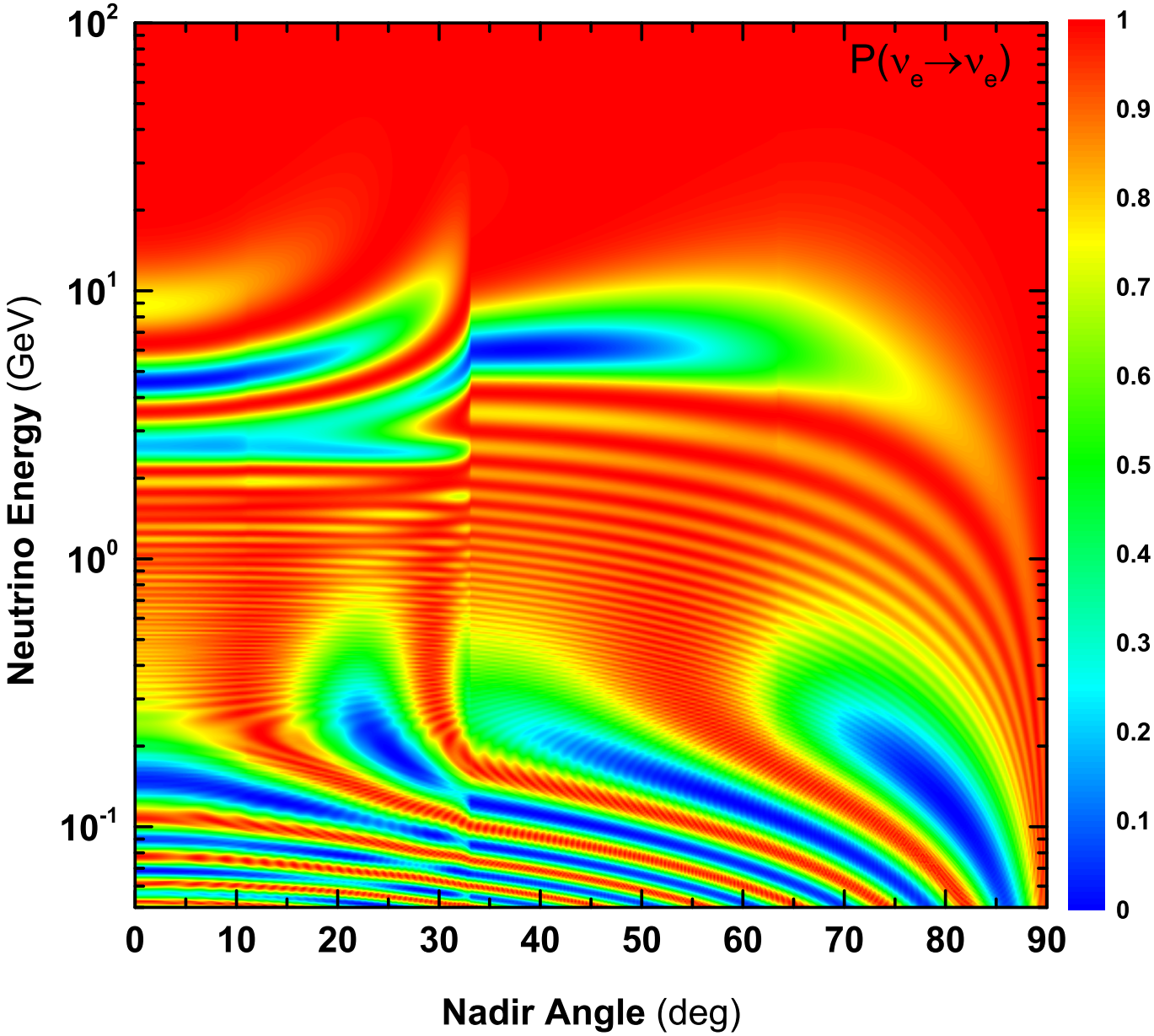

$e \to e$ oscillogram for NH.

Neutrino spectra

Top:NH.

Bottom:
IH/NH.

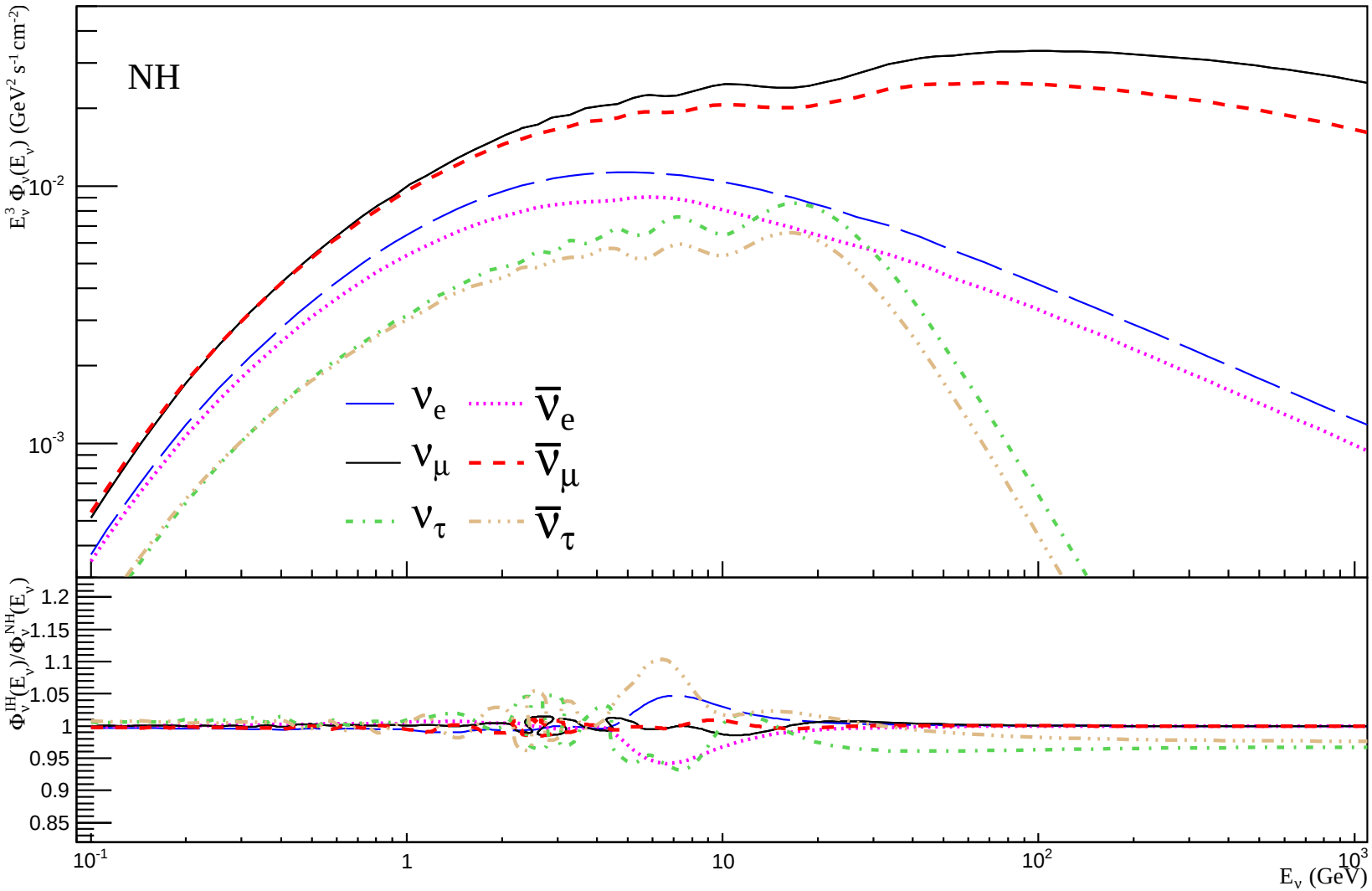

Flavor transition modulated angle averaged energy spectra of atmospheric neutrinos at the Kamioka site.

QES event rates in Super-Kamiokande

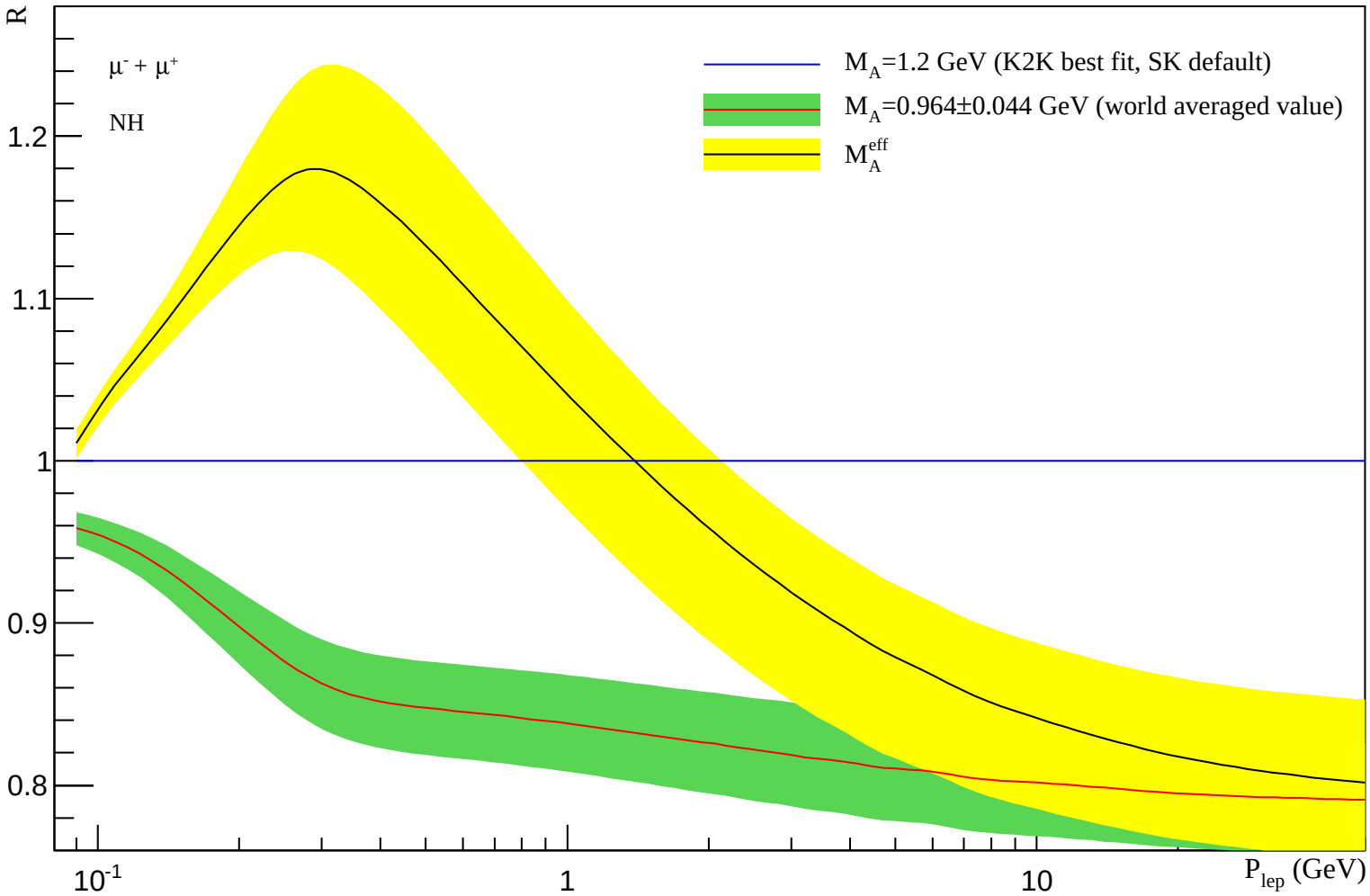

Muon QES event rates in the SK detector evaluated with several values of constant M_A and normalized to the rates calculated with the M_A^{eff}.

The calculations are done for NH.